Reducing Non-exhaust Emissions from the City of Vancouver's Light-duty Fleet

Prepared by: Mehmud Iqbal

UBC Sustainability Scholar, 2021

Prepared for: Leah Suley

Engineering Assistant – Operations Support

Fleet & Manufacturing Service, City of Vancouver

August 2021

This report was produced as part of the Greenest City or Healthy City Scholars Program, a partnership between the City of Vancouver and the University of British Columbia, in support of the Greenest City Action Plan and the Healthy City Strategy.

This project was conducted under the mentorship of City staff. The opinions and recommendations in this report, and any errors, are those of the author, and do not necessarily reflect the views of the City of Vancouver or The University of British Columbia.

The following are official partners and sponsors of the Greenest City or Healthy City Scholars Program:

Acknowledgements

I am humbly thankful that I live and work on the unceded homelands of the xʷməθkʷəy̓əm (Musqueam), Sḵwx̱wú7mesh (Squamish), and səlilwətaɬ (Tsleil-Waututh) nations

I would like to thank the following individuals for their contribution, feedback, and support throughout this project.

City of Vancouver

1. Leah Suley, EA – Operations Support, Fleet & Manufacturing Services
2. Rob Veer, Senior Mechanical Engineer – Maintenance & Engineering Support, Fleet & Manufacturing Services
3. Evan Dacey, Acting Branch Manager – Fleet Strategy and Asset Management, Fleet & Manufacturing Services
4. Sarah Labahn, Planning Analyst, Planning, Urban Design & Sustainability

University of British Columbia

1. Karen Taylor, Program Manager, UBC Sustainability Initiative

Cover photo by Takashi Miyazaki on Unsplash

Contents

List of Figures

List of Tables

Executive Summary

Non-exhaust emissions (NEE) of particulate matter (PM) from tire, brake, and road pavement, as well as resuspension of already deposited road dust, account for up to 90% by mass of total traffic-related PM emitted. These emissions arise regardless of the type of vehicle and its mode of power and contribute to the total ambient particulate matter burden associated with human ill-heath and premature mortality. While significant technological improvements have been made for reducing particulate matter from exhaust emissions, no actions are currently in place to minimize the non-exhaust part of emissions.

This report aims at measuring the PM2.5 and PM10 emissions generated in a month from tire wear and brake wear from the light-duty fleet of the City of Vancouver (CoV). The literature on measuring this emission quantity presents highly variable results due to the heterogeneity of NEE sources and the absence of standardized sampling and measurement protocols. As evidence, emission factors (EFs) for total PM were found to range from 0.3 mg km^{-1} veh^{-1} to 7.4 mg km^{-1} veh^{-1} for tire wear and from 1 mg km^{-1} veh^{-1} to 18.5 mg km^{-1} veh^{-1} for brake wear. This report utilized the emission factors used by USEPA in the latest version of Motor Vehicle Emission Simulator (MOVES) software. The results indicated that monthly 0.934 kg of PM2.5 and 6.226 kg of PM10 airborne emission are generated from tire wear, and another 1.840 kg of PM2.5 and 14.745 kg of PM10 are coming from the break wears. Several technical recommendations are made to address the tire wear and brake wear emissions, such as introducing air ducts for cooling of tire surface, improving asphalt materials. The replacement of internal combustion engine vehicles with electric vehicles (EV) is also considered a prevention strategy. However, there are still concerns regarding the increase of NEE deriving from the extra weight of the batteries. Other non-technological mitigation strategies, such as street washing or sweeping, changing driving behavior, and improving public transport to minimize vehicles on the road, have also proved effective in reducing PM levels.

The data reported in this report highlighted the need for future studies to broaden their research area and focus not only on the standardization of methods and the introduction of regulations but also on improving already existing technologies and mitigating strategies.

1.0 Introduction

Road traffic has long been viewed as a significant contributor to urban air pollution. Emissions of particulate matter from motor vehicles originate from two primary sources: the combustion of fossil fuel, which is emitted via tailpipe exhaust, and from non-exhaust processes, including the degradation of vehicle parts and road surfaces and the resuspension of road dust. The airborne particulate emissions generated by these processes are defined as non-exhaust PM emissions. Particulate matter is recognized as one of the main risk factors for adverse health effects and premature deaths worldwide (Brauer, et al., 2012). PM10 is the inhalable fraction and includes particles that enter the body through the nose and mouth when breathing; PM2.5 is the thoracic fraction and is composed of particles that penetrate the lungs under the larynx (Anenberg, et al., 2014; Kelly & Fussell, 2012). Tian et al. (2021) identified a highly toxic quinone transformation product of N-(1,3-dimethylbutyl)-N′-phenyl-p-phenylenediamine (6PPD), a globally ubiquitous tire rubber antioxidant, in the analysis of representative roadway runoff and stormwater-affected creeks of the US West Coast. The high presence of 6PPD in the creek water caused acute mortality when adult Pacific Northwest coho salmon (*Oncorhynchus kisutch*) migrate to urban creeks to reproduce.

Exhaust emissions (EE) mainly contribute to the fine (PM2.5 and PM10) and ultrafine (PM0.1) fractions of particulate matter. On the other hand, non-exhaust emissions (NEE) mainly contribute to PM10 and, to a lesser extent, to PM2.5 (Pant & Harrison, 2013; Timmers & Achten, 2016). In terms of chemical composition, primary EE contains a variety of hydrocarbons and combustion by-products. In contrast, NEE is mainly composed of heavy metals, such as zinc (Zn), copper (Cu), iron (Fe), and lead (Pb) (Almeida, et al., 2020; Thorpe & Harrison, 2008; Timmers & Achten, 2016). The volatile organic compounds in EE react with sunlight and form organic secondary aerosols, whereas NEE mainly produces secondary inorganic aerosols.

To quantify the release of PM into the environment, emission factors (EFs) are used as a tool to estimate the contribution of individual vehicles or vehicle fleet mixtures. They are typically derived for each category of vehicles (passenger cars, heavy-duty vehicles, etc.) and depend on various parameters (brake type, materials, driving style, vehicle weight, etc.). EFs from non-exhaust emissions can be estimated with three different methods, namely 1) direct measurements, 2) receptor modeling, and 3) emission inventories (Timmers & Achten, 2016). Emission inventories are the most reliable and comprehensive data sources since they derive from the compilation and analysis of a wide range of studies. Authoritative environmental agencies have developed guidelines to standardize the compilation of such inventories, e.g., the EMEP/EEA Air Pollutant

Emissions Inventory Guidebook (EEA, 2019) from the European Environment Agency and the "Procedures for Emission Inventory Preparation" from the United States Environmental Protection Agency (USEPA, Procedures of Emission Inventory Preparation- Volume IV: Mobile Sources, 1992). Therefore, they are the fundamental tools for air quality management and the correlation of human activities with the corresponding emissions of pollutants.

To regulate emissions from different sources and prescribe limits to be respected for vehicles produced after a certain year, international authorities set thresholds of emission factors (European Community, 2008). The European Union started defining the EURO standards for exhaust vehicle emissions in 1992 with EURO 1 (140 mg km^{-1} veh^{-1} for diesel cars). Since then, the threshold was progressively decreased, e.g., EURO 3 (the year 2000) brought the emission limit to 50 mg km^{-1} veh^{-1} for diesel cars. The current European emission threshold for exhaust PM emissions is 5 mg km^{-1} veh^{-1} for both diesel and gasoline cars, imposed with EURO 5 (since September 2009) and confirmed by EURO 6 (since September 2014). Similarly, the USA has been setting the TIER standards since 1991 (USEPA, All EPA Emission Standards Light-Duty Vehicles and Trucks and Motorcycles, 2020). These stringent regulations fostered the technological upgrade of combustion control and tailpipe emission treatment systems, thus leading to a dramatic decrease in the contribution of vehicle exhaust emissions to PM levels. However, non-exhaust emissions from traffic still represent a relevant PM10 and PM2.5 source in urban environments. As shown in Figure 1, the share of NEE on the total emissions from traffic is comparable or even exceeds the contribution of EE (Amato, et al., 2014). The relative contribution of NEE is expected to grow due to the reduction of exhaust emission factors steadily, the phase-out of most polluting cars, the progressive increase of EVs, and the lack of limiting standards for NEE (Hooftman, Messagie, Van Mierlo, & Coosemans, 2018).

Figure 1 Relative contribution of exhaust and non-exhaust emissions to total PM10 and PM2.5 emissions from road traffic, based on the research works

According to estimates reported by (OECD, 2020), the total amount of non-exhaust particulate matter (PM2.5) emitted by passenger vehicles worldwide is likely to rise by 53% by 2030 from a 2017 baseline, mainly due to increased vehicle mileage.

2.0 Types of Non-exhaust Emission

Non-exhaust emissions of particles arise mainly from four separate sources. Three of these arise from abrasion: tire wear, brake wear, and road surface wear. The fourth, particle resuspension, arises from road dust particles being suspended into the atmosphere by passing traffic. All these emission types are generated by battery-electric vehicles as well as internal combustion engine vehicles. Although their magnitude may change, road traffic will continue to be a source of particulate matter, even for a fully electric vehicle fleet. The scope of this report will be limited to the particulate matter emissions generated by tire wear and brake wear.

2.1 Tire wear

The tire is a complex elastic rubber product that is the only part of a vehicle that contacts the ground. A tire structure mainly includes tread, tire shoulder, tire side, belt ply, cord ply, inner lining, etc., as shown in Figure 2. The wear process of tires is relatively complex. Still, there are three main influencing factors: tire factors (structure, material, wear resistance, etc.), vehicle factors (suspension parameters, load, speed, driving force, etc.), and environmental factors (road conditions, temperature, driving habits, etc.). In the contact process between tires and ground, there are direct friction and slippage, which causes micro-cutting and tearing between tires and road surface. In this process, the wear between tires and ground exists all the time. When the accumulated friction energy of a local volume in the contact area reaches the failure energy (critical value) of the tire surface in the contact area, the local volume will be removed from the surface in the form of abrasive chips, namely, wear appears. However, tires wear usually does not exist in a single form, but in mixed wear between tires and road surface, each accounting for about 50% (Faino, 2018). The tire wear particles will be released into the air, road surface, soil, or rivers. Figure 3 shows a scanning electron microscope image of the tire wear generated.

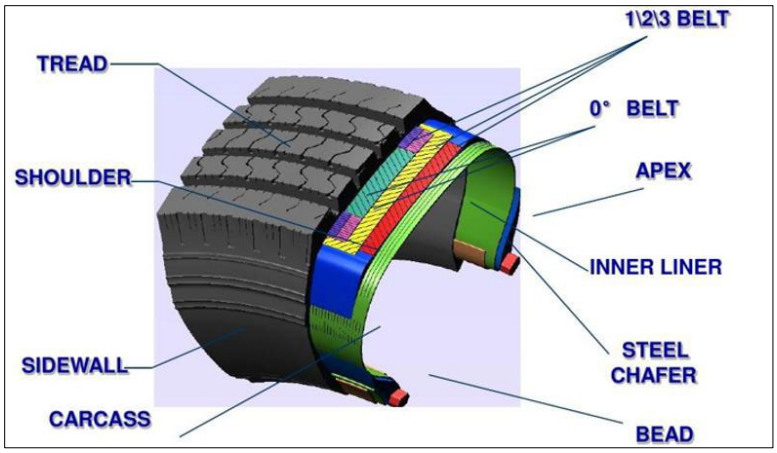

Figure 2 The structure of a tire

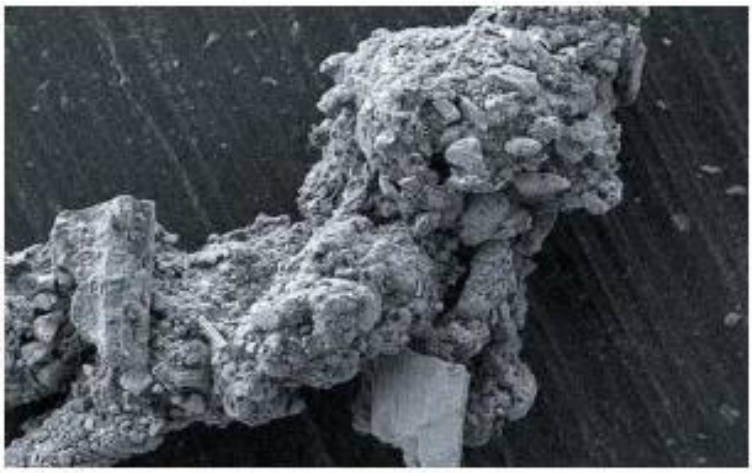

Figure 3 Physical characteristics of tire wear particles

Heavy braking and accelerating (including turning and road grade) significantly increase tire wear. The route and style of driving determine the amount of acceleration. Highway geometry is a crucial factor, with rising and falling in roads resulting in increased tread wear. The acceleration of the vehicle determines the forces applied to the tire and includes turning. Tire wear due to tire/road interface is determined by and is directly proportional to these forces. The season results in temperature, humidity, and water contact variations. Wear rates are lower in wet compared to dry conditions. Finally, vehicle characteristics also influence tire wear. Key factors are the weight, suspension, steering geometry, and tire material and design. Axle geometry changes result in uneven wear across the tire width. The type of tire influences the wear significantly, in particular, the physical characteristics like the shape of the tire (determined by stiffness), the rubber volume (tread pattern), and the characteristic of the tire (rubber type, etc.). Because of different manufacturing specifications, different brands of tires wear at different rates.

2.2 Brake wear

Two brake system configurations have been widely used in modern passenger vehicles: disc brakes, in which flat brake pads are forced against a rotating metal disc (Figure 4), and drum brakes, in which curved brake shoes are forced against the inner surface of a rotating cylinder. Modern passenger vehicles are usually equipped with disc front and either disc or drum rear brakes, while in the past, drum brakes were generally employed as rear brakes. It is estimated that front brakes must provide approximately 70% of total braking power and therefore must be replaced more frequently than rear ones. Most car braking systems consist of frictional pairs made of a disc, a pad, and a caliper. Figure 4 depicts a disc brake assembly with a single-piston floating caliper and a ventilated rotor (Wahlström, 2009). Rotors used in passenger vehicles are usually made of grey cast iron. Still, they can be made of composites, such as reinforced carbon-carbon, ceramic matrix composites, and aluminum in some cases.

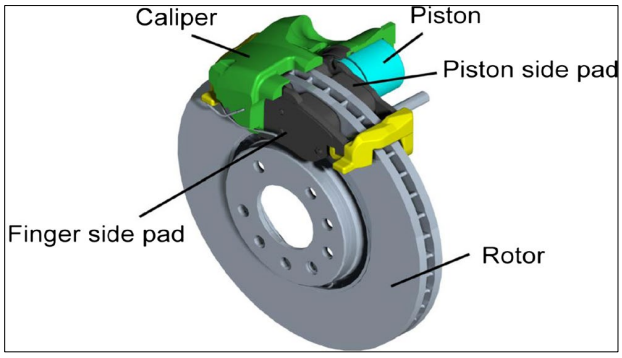

Figure 4 Graphic representation of a disc brake system

Three different lining types are usually found in passenger vehicles: non-asbestos organic (NAO), semi-metallic, and low metallic. NAO-type pads are relatively soft and exhibit low brake noise compared to other types of pads, but they lose braking capacity at high temperatures and create more dust than the other types. For many years, brake linings were composed of asbestos fibers, while today, they are asbestos-free due to serious health concerns (Thorpe & Harrison, 2008). Canada was once a world leader in asbestos production; however, the Canadian government banned asbestos effective from 30 December 2018, making it illegal to import, manufacture, sell, trade, or use products made with the toxic mineral. Low-metallic pads comprise organic compounds mixed with small amounts of metals (10– 30 % by mass). They exhibit high friction and good braking capacity at high temperatures. Semi-metallic brake pads have higher metallic content (up to 65% by mass), making them more durable and with excellent heat transfer. On the other hand, they tend to wear down rotors faster and exhibit intrusive noise characteristics. For high-

performance requirements, or extreme braking conditions (sports cars, ambulances, police cars), metallic linings which contain steel and copper fibers are employed.

The frictional contact between the disc and the pad generates particles of various sizes. The mass size distribution of brake wear particles heavily depends on vehicle speed, deceleration, inertia, and the composition of brake materials. Since mechanical wear is the main PM generation process, the distribution mode is generally observed to be above 1 µm (Sanders, Xu, Dalka, & Maricq, 2003). The caliper acts mechanically on the pad during a braking event, which slides against the disc and transforms vehicle kinetic energy into thermal energy. Apart from the mechanical abrasion, vehicle brakes become subject to sizeable frictional heat generation with subsequent wear of linings and rotors. This generates mostly micron-sized particles. Figure 5 shows particles of different sizes generated due to brake wear tests performed in the laboratory (Kukutschová, et al., 2011).

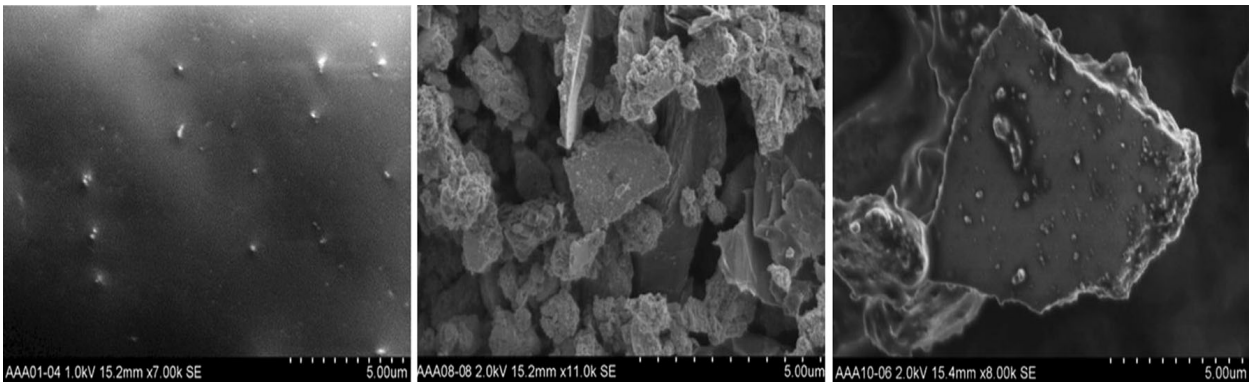

Figure 5 Scanning Electron Microscope images of brake wear particles (left <56 nm, middle PM2.5, right PM10)

Not all wear debris generated during braking becomes airborne. Approximately 50% of wear particles are smaller than 20 µm diameter, while almost 40% of brake wear debris is emitted as PM10 (Garg, et al., 2000; Sanders, Xu, Dalka, & Maricq, 2003). The rest may deposit on the road surface or be attracted to the vehicle with its fate remaining unknown. The highest concentrations of brake wear particles are observed near busy junctions, traffic lights, pedestrian crossings, and corners, even if wear particles may also be released from the brake mechanism sometime after the primary emission event. Several studies within the urban environments have reported the contribution of brake wear particles to non-exhaust traffic related PM10 emissions ranging between 16 and 55% by mass (Harrison, Jones, Gietl, Yin, & Green, 2012). These reports also found significantly lower contributions (~3 % by mass) in highways where braking events are less frequent (Bukowiecki, et al., 2009).

Additionally, studies have revealed contributions of brake wear to total traffic-related PM10 emissions of 11–21 % by mass (Lawrence, et al., 2013). On the other hand, brake wear contributions to ambient PM10 concentrations vary from negligible to up to 4 μg m^{-3} (Amato, et al., 2009). There is a general decrease in engine exhaust emissions due to catalytic converters, diesel particulate filters (DPF), and improved fuels and engines. It is expected that the relative contribution of brake wear particles to the total PM levels will increase in the forthcoming years (Amato, et al., 2014).

2.3 Other types of non-exhaust emission

Road surface wear

Road surfaces are typically concrete-based or asphalt-based: the former is made of coarse aggregate, sand, and cement, while the latter is mainly composed of mineral aggregate (95%). The remaining 5% is composed of bitumen, a highly viscoelastic black blend of hydrocarbons and their derivatives obtained from the fractional distillation of crude oil. The road surface is a relevant source of both primary and secondary PM in urban areas. The former originates from the fragmentation of the road pavement surface due to the interaction with vehicle tires. The friction between tire and road surface leads to the abrasion of road surface and the consequent release of airborne particles in the environment. The secondary aerosol derives from transforming the organic asphalt-based materials released in the air during the road wear process (Khare et al., 2020).

The chemical characterization of the wear particles is difficult to perform due to the complex composition of the road mixtures. Abundant stone fractions in the pavement result in mineral wear mainly composed of Si, Ca, K, Fe, and Al (Lindgren, 1996). Moreover, dust particles with similar mineralogical compositions are released from other sources, such as construction sites and winter sanding/salting. As the dust from these sources' deposits onto the road surface and is resuspended by wind or vehicle-induced turbulence, it becomes challenging to identify particulate from road wear (Gehrig, et al., 2010).

Resuspended road dust

Most of the non-exhaust particles derive from the resuspension of material already deposited on the road surface (between wheel tracks, on the curbside, or into the pores of the asphalt) due to tire shear, vehicle-generated turbulence, and the action of the wind. Therefore, the terms 'road

dust', 'road sediments,' or 'street dust' include any form of a solid particle on the road surface that can be suspended in the atmosphere through traffic or windblown action (Denby, Kupiainen, & Gustafsson, 2018). Only particles with a size below 70 µm can be airborne; however, all the deposited dust can be resuspended as larger particles may be ground into finer ones by the vehicle weight.

Several sources contribute to road dust: deposited brake/tire/road wear particles, deposited particles from exhaust emissions, particles from nearby environments, fugitive loading from constructions, roadsides and/or unpaved roads, dry and wet deposition from the atmosphere, application of salt during freezing periods, traction sand, deposition of pollen and plant materials (Amato, et al., 2014). The dominant contributor to road dust largely varies according to the environment: in colder regions, the predominant source is the road wear from studded tires (Norman & Johansson, 2006), in urban environments, the relevant sources are tire and brake wear (Bukowiecki, et al., 2010), while in some cases there may be no dominant source. Because of the heterogeneity of dust sources, it is difficult to distinguish between "direct" wear emissions (tire, brake, or road wear) and "resuspended" wear emissions, and therefore to separate their relative contribution to atmospheric PM levels (Denby, Kupiainen, & Gustafsson, 2018). Road dust has natural or anthropogenic origins, and its composition varies depending on geographical location, climate factors, resuspended soil, and anthropogenic sources (Candeias, et al., 2020).

3.0 Emission Factor Benchmarking Methodology

3.1 Tire wear emission factor

According to the literature, the most straightforward method for determining tire wear is the periodic measurement of tread depth. However, variations in the extent of wear across the tire and irregularities in tire shape could lead to inaccurate measurements. Determining tire weight loss is a more sensitive approach than the measurement of tire depth. However, care must be taken to avoid errors due to damage to tires during removal from the vehicle and hubs and materially embedded in the tire. To minimize damage to the tire, (Lowne, 1970) weighed both the wheel and tire simultaneously after the wheel was brushed and stones embedded in the tire were removed. Tire wear rates have been measured and estimated for a range of vehicles from passenger cars to light and heavy-duty trucks, with results reported either as emissions per tire or per vehicle. Most of the studies report only wear, not airborne PM. The wear rates found in the literature are summarized in Table 1 below (USEPA, Brake and tire wear emissions from on-road

vehicles in MOVES3, 2020) and are converted to a per-vehicle rate (units are in per vehicle kilometer). A range of light-duty tire wear rates from 64-360 mg/vehicle/km has been reported in the literature. Much of the variability in these wear rates can probably be explained by the factors such as tire lifetime in kilometers traveled, initial weight, tread surface depth, and speed variation.

Table 1 Tire wear rates found in the literature per vehicle

Source	Remarks	Rate in mg km^{-1} veh^{-1}
Kupiainen, K.J. et al. (2005)	Measured tire wear rate	9 mg/km- PM_{10}
		2 mg/km-$PM_{2.5}$
Luhana et al. (2003)	Measured tire wear rate	74
Councell, T.B. et al. (2004) US Geological Survey	Calculated rate based on literature	200
Warner et al. (2002)	Average tire wear for a vehicle	97
Kolioussis and Pouftis (2000)	Average estimated tire wear	40
EMPA (2000)	Light duty vehicle tire wear rate	53
	Heavy-duty vehicle tire wear rate	798
SENCO (Sustainable Environment Consultants Ltd.) (1999)	Light duty vehicle tire wear rate	53
	Wear rate for trucks	1403
Legret and Pagotto (1999a)	Estimated rate for light duty vehicles	68
	Estimated rate for heavy vehicles (>3.5t)	136
Baumann (1997)	Passenger car tire wear rate	80
	Heavy-duty vehicle tire wear rate	189
	Articulated lorry tire wear rate	234
	Bus tire wear rate	192
Garben (1997)	Passenger car tire wear rate	64
	Light duty vehicle tire wear rate	112
	Heavy duty vehicle tire wear rate	768
	Motorbike tire wear rate	32
Gebbe (1997)	Passenger car tire wear rate	53
	Light duty vehicle tire wear rate	110
	Heavy duty vehicle tire wear rate	539
	Motorbike tire wear rate	26.4

Schuring and Clark (1988)	Estimated tire wear rate	240-360
Pierce, R.N. (1984)	Estimated tire wear rate	120
Malmqvist (1983)	Estimated tire wear rate	120
Gottle (1979)	Estimated tire wear rate	120
Cadle et al. (1978)	Measured tire wear rate	4
Dannis (1974)		90

The methodology of tire wear emission factor followed by USEPA primarily depends on the data from work published by Luhana et al. (2004), wherein wear loss rates for tires have been determined gravimetrically for in-service cars. The authors weighed car tires at two-month intervals and asked drivers to note the details of each trip undertaken. Five test vehicles (labeled A-E) were selected for the tests. Of these vehicles, A (1998 Audi A3), B (1994 Ford Mondeo), C (1990 Peugeot 205), and E (1992 Vauxhall Cavalier) were front-wheel drive vehicles (FWD). According to the driver surveys, the predominant road type used by vehicles A and B were motorways. For vehicle D (1990 Ford Sierra), it was rural roads and motorways; for vehicle C, it was suburban roads; and vehicle E, it was rural roads. Vehicle D was excluded from this study since it was a rear-wheel-drive (RWD) vehicle. RWD vehicles are relatively uncommon amongst passenger vehicles in the United States, and the wear from this vehicle was more than double the other FWD vehicles. It is uncertain whether the discrepancy from this vehicle was because it was a rear-wheel-drive or for some other reason. The selection of vehicles was based primarily on driving conditions, as defined by the primary type of road used by the owner and annual distance driven.

Results from the Luhana et al. (2004) study indicated that the lowest tire wear rates (56 mg km^{-1} veh^{-1} and 67 mg km^{-1} veh^{-1}, respectively) were for vehicles A and B that were driven predominantly on motorways. Vehicles C and E had very similar wear rates (around 85 mg km^{-1} veh^{-1}), although these vehicles tended to be driven on different roads. Based on the wear rates from the four front-wheel-drive cars alone, the study concluded that the average wear rate is around 74 mg km^{-1} veh^{-1}. This value is in the lower end of the range of wear rates reported in the literature.

The data presented in Table 2 includes calculations for the distances completed by each vehicle between successive tests, the estimated average trip speeds, and predominant road types for the equivalent periods. It was assumed that the weight of the wheels remained constant during the tests, and any weight loss was due solely to the loss of tire rubber during driving.

Table 2 Data from Luhana et al. (2004) with measurements of tire wear for a variety of trips

	Avg. trip speed	Tire Wt. Loss (per axle)		total wt. loss (per vehicle)	avg. speed
vehicle tests	km/hr	Front mean (g/km)	Rear Mean (g/km)	g/km	mi/hr
test1-A	90.3	0.0202	0.0092	0.0589	56.1
test2-A	90.6	0.0209	0.0126	0.0669	56.3
test3-A	93.9	-	0.0069	-	58.4
test4-A	92.7	0.0172	0.0086	0.0516	57.6
test1-B	65.4	0.0298	0.0087	0.077	40.6
test2-B	71.9	0.0262	0.0091	0.0705	44.7
test3-B	74.4	0.019	0.004	0.0461	46.2
test4-B	70.2	0.0297	0.007	0.0735	43.6
test1-C	44.5	0.0312	0.0047	0.0718	27.7
test2-C	42.9	0.0331	0.0132	0.0925	26.7
test3-C	48.8	0.0284	0.0064	0.0697	30.3
test4-C	50.4	0.0532	0.0045	0.1153	31.3
test3-E	61.3	0.037	0.0104	0.0948	38.1
test4-E	65.8	0.0265	0.0109	0.0749	40.9

Using the above data on average speed and total weight loss, an exponential regression curve was fitted, characterized by an R^2 value of 0.43. The actual and predicted values are presented in Figure 6 (USEPA, Brake and tire wear emissions from on-road vehicles in MOVES3, 2020).

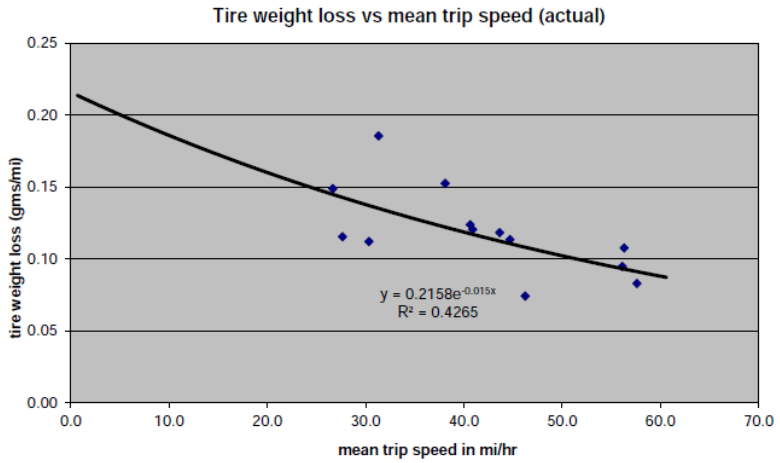

Figure 6 Relationship between light-duty tire weight loss (per vehicle) and mean trip speed

It can be seen from the curve in Figure 6 that the wear approaches a maximum at zero speed and goes down as the speed goes up. This is based on the extrapolation of the fitted curve. It may seem counter-intuitive that emissions are highest when speed nears zero; however, it is essential to note that acceleration and turning have not been accounted for. Much of the tire wear occurs when the magnitude of a vehicle's acceleration/deceleration is at its greatest, e.g., at low speeds when the vehicle is accelerating from rest or when the vehicle is braking hard to stop.

Once the average tire wear was quantified, it was necessary to determine the fraction of that wear that becomes airborne PM. The literature indicates that probably less than 10 percent of car tire wear is emitted as PM10 under 'typical' driving conditions, but the proportion could be as high as 30 percent (Warner, Sokhi, Luhana, Boulter, & McCrae, 2004). According to Luhana et al. (2004), PM10 is released from all four tires at a rate of between 4 and 6 mg km^{-1} veh^{-1} for passenger cars. This suggests that generally, between 1% and 15% by mass of passenger car tire wear material is emitted as PM10 (though much higher proportions have been reported in some studies). USEPA assumed that 8% of tire wear is emitted as PM10 (average of 1% and 16%).

According to Kupiainen et al. (2005), PM2.5 fractions were on average 15% of PM10. This study assumes that 1.2% of the total tire wear is emitted as PM2.5 to develop the tire wear emission rate. The 1.2% is derived from assuming that 8% of tire wear is to be emitted as PM10 and 15% of PM10 is PM2.5.

USEPA applies the same tire wear emission rate for all vehicle fuel types (gasoline, diesel, flex-fuel, CNG, or electric) within a regulatory class. The average PM2.5 and PM10 tire wear emission rates for each regulatory class, across road types, from a national scale, run for the calendar year 2017 using MOVES3 is shown in Table 3 (USEPA, Brake and tire wear emissions from on-road vehicles in MOVES3, 2020).

Table 3 Average PM2.5 and PM10 tire wear PM emission rates for the MOVES regulatory classes from a national scale run inventory for the calendar year 2017 using MOVES3

Type of vehicle	PM2.5		PM10	
	mg $mile^{-1}$ veh^{-1}	mg km^{-1} veh^{-1}	mg $mile^{-1}$ veh^{-1}	mg km^{-1} veh^{-1}
Motorcycle	0.64	0.40	4.29	2.66
Passenger Car	1.28	0.80	8.55	5.32
Passenger Truck	1.28	0.80	8.57	5.32
Light Commercial Truck	1.37	0.85	9.16	5.69
Intercity Bus	3.87	2.40	25.77	16.01
Transit Bus	2.35	1.46	15.68	9.74
School Bus	2.30	1.43	15.31	9.51
Refuse Truck	3.93	2.44	26.19	16.27
Single Unit Short-haul Truck	2.25	1.40	15.03	9.34
Single Unit Long-haul Truck	2.17	1.35	14.48	9.00
Motor Home	2.21	1.37	14.75	9.16
Combination Short-haul Truck	3.81	2.37	25.39	15.78
Combination Long-haul Truck	4.13	2.56	27.51	17.10

3.2 Brake wear emission factor

Brake wear is defined as the mass of material lost from the brake pads. A fraction of that wear becomes airborne. The composition of the brake liner influences the quantity and makeup of the released particles. Disc brakes are lined with brake pads, while drum brakes use brake shoes or friction linings. These materials differ in their wear rate, the portion of wear particles that become airborne, and the size and composition of those particles. The overall size or mass of the brake

pads also varies with vehicle type. Typically, trucks use larger brakes than passenger vehicles because their mass is greater.

There are a very limited number of publications on brake wear PM emissions. There are even fewer publications discussing size distributions and speciation and none quantifying emissions modally on which to base a model directly. Garg et al. (2000) conducted a study in which a brake dynamometer was used to generate wear particles under four wear conditions - at nominal temperatures of 100 °C, 200 °C, 300 °C, and 400 °C. The study was performed using seven brake pad formulations that were in high volume use in 1998. Measurements were taken on both the front disc as well as rear drum brakes. The study measured mass, size distribution, elemental composition, and fiber concentration at four temperature intervals. The report also estimated PM2.5 and PM10 emissions for light-duty vehicles of 3.4 and 4.6 mg/mile, respectively, for small vehicles, and PM2.5 and PM10 emissions of 8.9 and 12.1 mg/mile, respectively, for pickup trucks.

Sanders et al. (2003) looked at three classes of lining materials: low metallic, semi-metallic, and non-asbestos organic (NAO), representing about 90 percent of automotive brakes at that time. In their dynamometer tests, three lining type/vehicle combinations (low metallic/mid-size car, semi-metallic/full-size truck, and non-asbestos organic/full-size car) were subject to two sets of braking conditions: the urban driving program (UDP) with a set of 24 stops which represent relatively mild braking (≤ 1.6 m/s^2) at relatively low speed (<90 km/h); and the Auto Motor and Sport magazine (AMS) test representing harsh braking conditions consisting of 10 consecutive 7.9 m/s^2 stops from 96 km/h. In addition to the dynamometer tests, the authors also reported two other testing scenarios: (a) a wind tunnel test where a series of 1.8 m/s^2 stops from 96 km/h of a full-size car with low metallic brakes were conducted; (b) test track testing of the same vehicle where stops from 60 mph at 0.15, 0.25 and 0.35 g-forces were conducted with low metallic and NAO brakes. The major findings from those tests were:

- The mean particle size and the shape of the mass distribution are very similar for each of the three linings.
- The wear rates are material-dependent: the low metallic linings generate 3-4 times the number of wear particles compared to semi-metallic and NAO linings.
- 50-70% of the total wear material was released in the form of airborne particles.
- The wear (and portion of wear that is airborne PM emissions) increased non-linearly with higher deceleration levels.
- The most abundant elements in brake wear debris composition were Fe, Cu, Si, Ba, K, and Ti, although the relative composition varied significantly by brake type.

Table 4 contains the emission rates derived from the literature review conducted. While emission rates are presented from other papers, USEPA largely relies on the Sanders et al. (2003) article, as it includes the most comprehensive array of materials in use at the time of analysis, measurement techniques, and deceleration ranges in a scientifically designed study. It is the only paper from which modal rates can be derived. The other papers' results are provided as a source of comparison.

Table 4 Literature values of emission factors from brake lining wear per vehicle

Literature Source	Vehicle Type	PM2.5 [mg/km]	PM_{10} [mg/km]
Luhana et al. (2004)	Light Duty		0-79
	Heavy Duty		0-610
Sanders et al. (2003)	Light Duty		1.5-7.0
Abu- Allaban et al. (2003)	Light Duty	0- 5	0-80
	Heavy Duty	0-15	0-610
Westurland (2001)	Light Duty		6.9
	Heavy Duty		41.2
Garg et al (2000)	Passenger Cars	3.4	4.6
	Large Pickup Trucks	8.9	12.1
Rauterberg-Wulff (1999)	Passenger Cars		1.0
	Heavy-Duty Vehicles		24.5
Carbotech (1999)	Light Duty		1.8-4.9
	Heavy Duty		3.5
Cha et al. (1983) used in PART5	Cars and Trucks		7.8

The analysis for USEPA braking emission rates is based on the following assumptions (USEPA, Brake and tire wear emissions from on-road vehicles in MOVES3, 2020):

1. An equal mix of the three brake types.
2. Four brakes per light-duty vehicle, including two front disc brakes and two rear drum brakes.
3. 2/3 of braking power (and thus emissions) in front brakes and 1/3 in the rear.
4. The fraction of total PM below 2.5 µm is ~ 10% (+/-5%).
5. 60% of brake wear is airborne PM (+/- 10%).

6. Same brake wear emission rate for all vehicle fuel types (gasoline, diesel, flex-fuel, CNG, or electric) within a MOVES regulatory class.
7. The PM10/PM2.5 ratio is based on the assumptions that the mass fraction of particles below PM10 is 0.8, and the mass fraction of particles below PM2.5 is 0.1. These assumptions result in a PM10/PM2.5 ratio of 8.

Table 5 Average PM2.5 and PM10 brake wear PM emission rates for the MOVES source types from a national scale run inventory for the calendar year 2017 using MOVES3

Source Type	PM2.5		PM10	
	mg/veh-mile	mg/veh-km	mg/veh-mile	mg/veh-km
Motorcycle	1.58	0.98	12.61	7.83
Passenger Car	2.77	1.72	22.17	13.78
Passenger Truck	2.88	1.79	23.08	14.34
Light Commercial Truck	3.08	1.91	24.64	15.31
Intercity Bus	15.50	9.63	123.98	77.04
Transit Bus	9.45	5.87	75.62	46.99
School Bus	9.94	6.18	79.55	49.43
Refuse Truck	13.35	8.29	106.77	66.34
Single Unit Short-haul Truck	8.24	5.12	65.89	40.94
Single Unit Long-haul Truck	6.88	4.28	55.04	34.20
Motor Home	10.66	6.62	85.26	52.98
Combination Short-haul Truck	9.52	5.91	76.13	47.30
Combination Long-haul Truck	7.96	4.94	63.64	39.55

4.0 Light-duty Fleet Data

Data was collected for the kilometers driven by the light-duty fleet of the City of Vancouver in the month of April 2021. There is a total of 1,182 assets in the light-duty fleet, and those are classified into the following categories according to USEPA regulation:

Table 6 Types of vehicles in the light-duty fleet of the City of Vancouver

Regulatory class	# Of assets	Total monthly usage (km)
Motorcycle	41	14,310
Passenger car	532	552,782
Passenger truck	106	428,472
Light commercial truck	503	152,106
Total	**1,182**	**1,147,670**

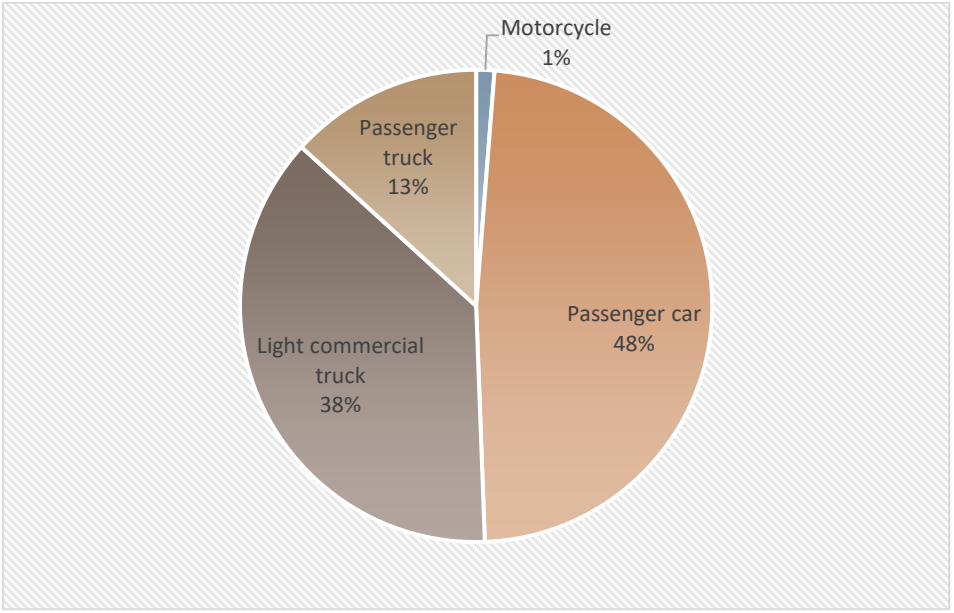

Figure 7 Kilometers driven by each type of vehicle of the light-duty fleet of the City of Vancouver

5.0 Results and Discussions

Based on the emission factor established in section 3 of this report, the airborne emission and total emission generated by the light-duty fleet of the City of Vancouver has been calculated for tire wear and brake wear based on the kilometers driven in April 2021.

5.1 Tire wear

Table 7 lists the estimated amount of airborne and total tire wear to the environment generated in April 2021 by the light-duty fleet of the City of Vancouver. The fleet emitted 0.934 kg of PM2.5 and 6.226 kg of PM10 as airborne emissions due to tire wear. At the same time, it is estimated that the total PM2.5 and PM10 emissions due to tire wear are 11.674 kg and 77.826 kg, respectively. These numbers are presented in Figures 8 & 9.

Table 7 Monthly emissions estimation from tire wear of CoV light-duty fleet

	# Of assets	Airborne Emission rate from tire wear		Total tire wear to the environment	
		$PM_{2.5}$ (kg)	PM_{10} (kg)	$PM_{2.5}$ (kg)	PM_{10} (kg)
Motorcycle	41	0.006	0.038	0.071	0.476
Passenger car	532	0.442	2.941	5.514	36.760
Light commercial truck	503	0.364	2.438	4.571	30.475
Passenger truck	106	0.122	0.809	1.517	10.115
Total	**1,182**	**0.934**	**6.226**	**11.674**	**77.826**

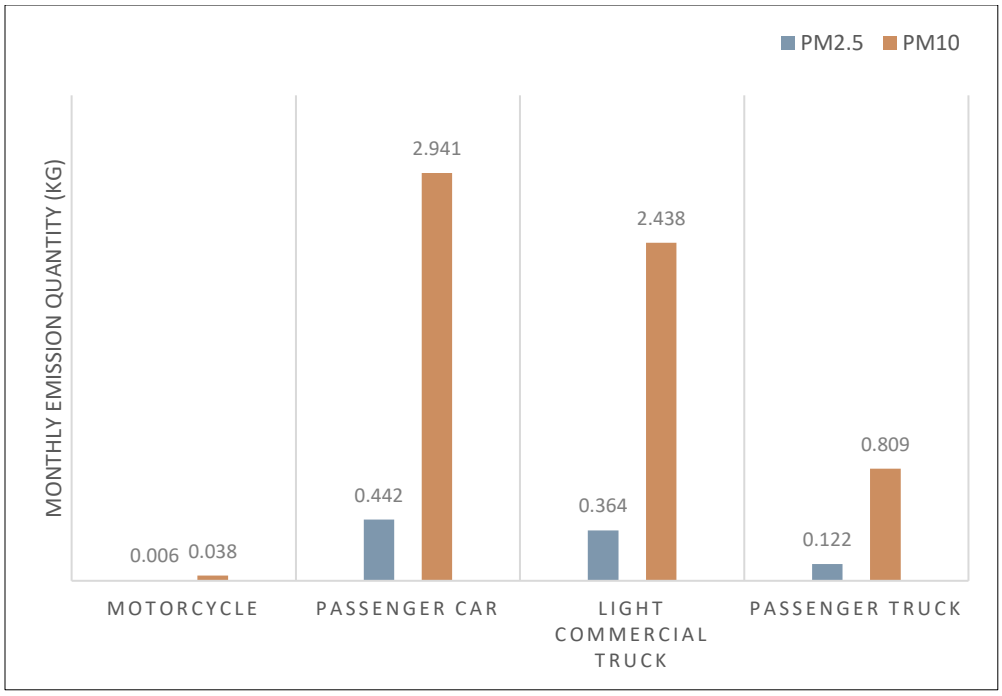

Figure 8 Airborne PM emission from tire wear of CoV light-duty fleet in April 2021

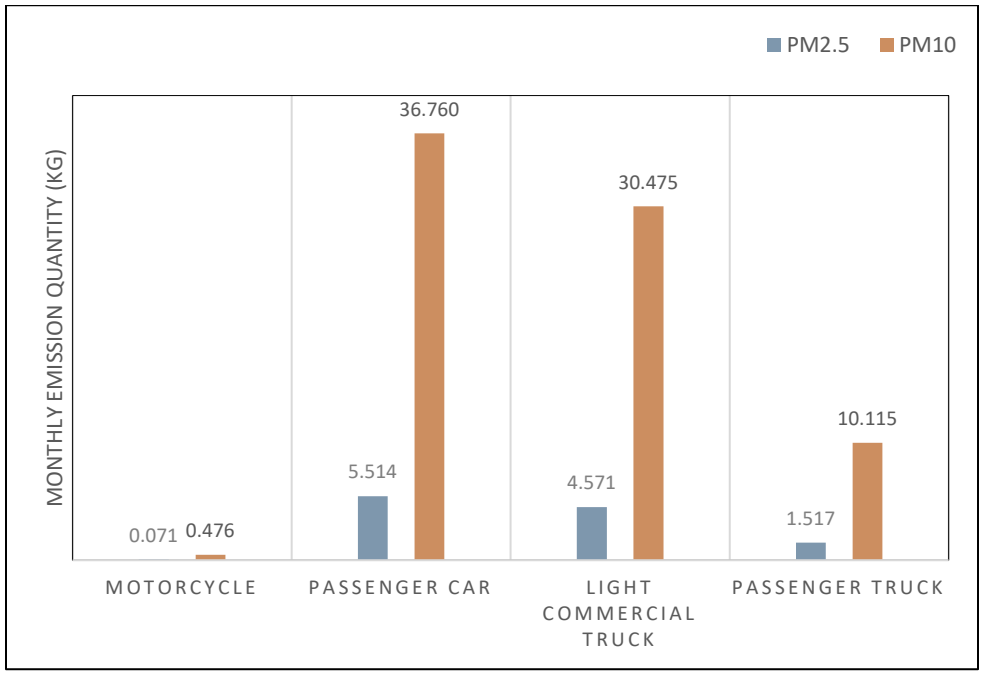

Figure 9 Total PM emission from tire wear of CoV light-duty fleet in April 2021

5.2 Brake Wear

Table 8 lists the estimated amount of airborne and total brake wear emissions to the environment that was generated in April 2021 by the light-duty fleet of the City of Vancouver. The fleet emitted 1.840 kg of PM2.5 and 14.745 kg of PM10 as airborne emissions due to brake wear. At the same time, it is estimated that the total PM2.5 and PM10 emissions due to break wear are 3.072 kg and 24.574 kg, respectively. It is to be mentioned that this calculation is based on assuming 66% less brake wear emission (Hooftman N. e., 2016) from the total 172 electric and hybrid vehicles that are present in the fleet with regenerative braking system.

Table 8 Monthly emissions estimation from brake wear of CoV light-duty fleet

	# Of assets	Airborne Emission rate from brake wear		Total brake wear emission to the environment	
		PM2.5 (kg)	PM10 (kg)	PM2.5 (kg)	PM10 (kg)
Motorcycle	41	0.014	0.108	0.023	0.181
Passenger car	532	0.775	6.207	1.293	10.345
Light commercial truck	503	0.817	6.551	1.365	10.919
Passenger truck	106	0.234	1.878	0.391	3.130
Total	**1,182**	**1.840**	**14.745**	**3.072**	**24.574**

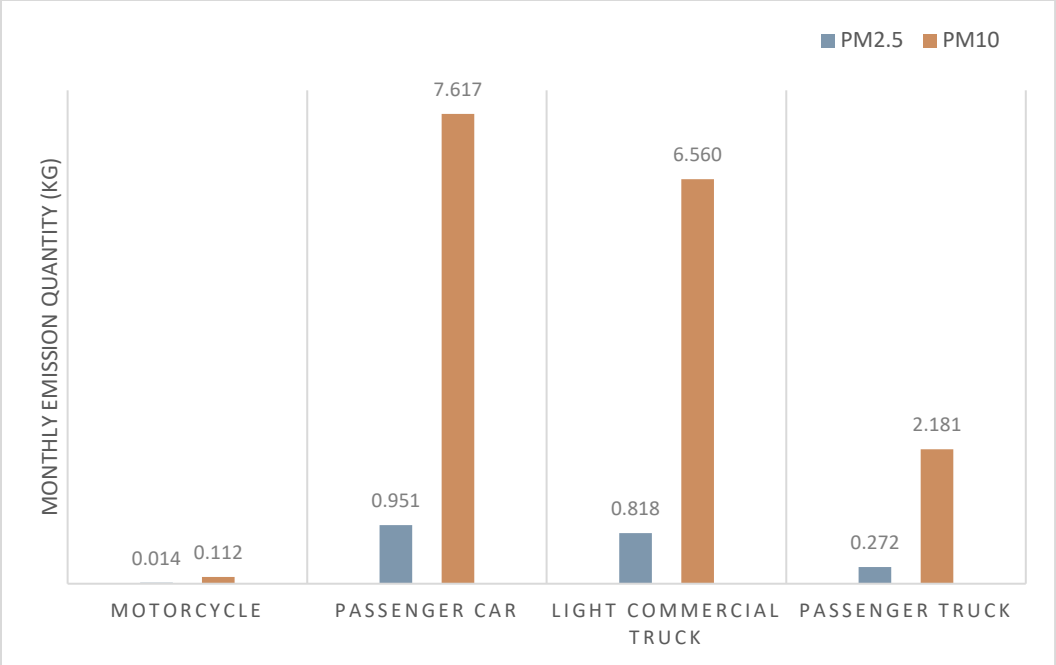

Figure 10 Airborne PM emission from brake wear of CoV light-duty fleet in April 2021

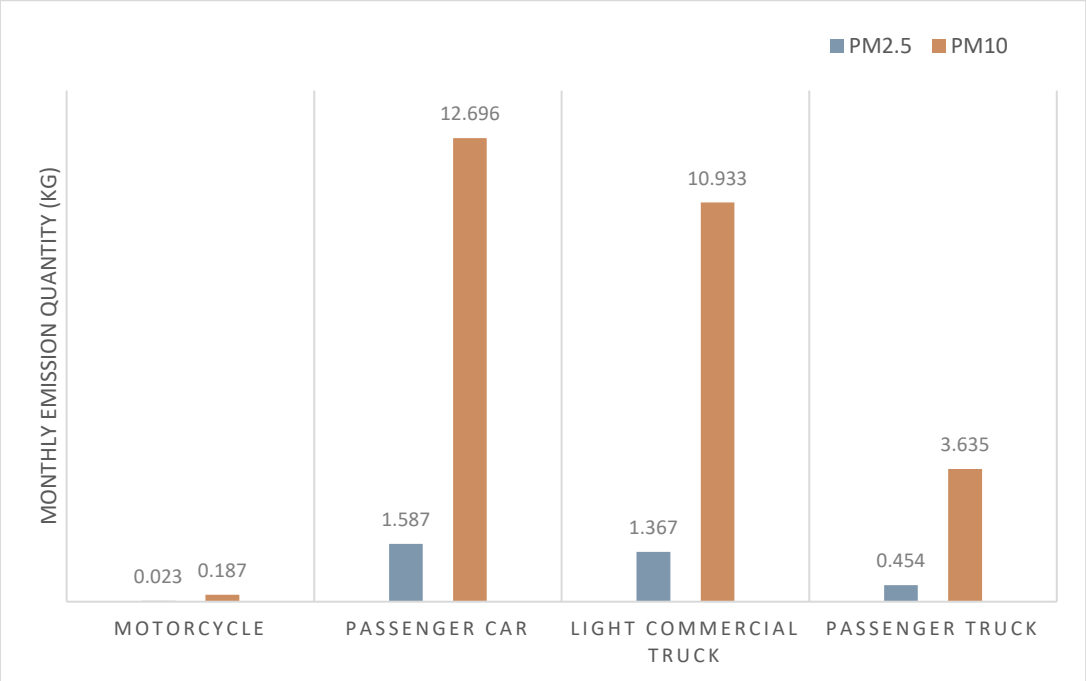

Figure 11 Total PM emission from brake wear of CoV light-duty fleet in April 2021

6.0 Recommendations

6.1 Technological measures

6.1.1. Air ducts for cooling of the tire surface

Park et al. (2019) evaluated the amount of fugitive dust generated during driving for different vehicle speeds. In addition, three different types of air ducts were installed in the front part of the vehicle, and the effect of cooling tires on the reduction in the fugitive dust generation was investigated. The temperature distribution on the tire surface was studied by simulation, and the amount of fine dust generated by tire wear was calculated with an empirical correlation. When an I-shaped duct was introduced, the average temperature of the tire surface was decreased by about 2-3 °C. As a result, the amount of generated fugitive dust was reduced by approximately 4.6%.

Model of three different types of air duct installed in a vehicle: (a) Y-type, (b) I-type, (c) S-type, as shown in Figure 12. These were designed to deliver the air to the tire through the high duct. Direct air supply to the front of the tire is most advantageous for tire cooling.

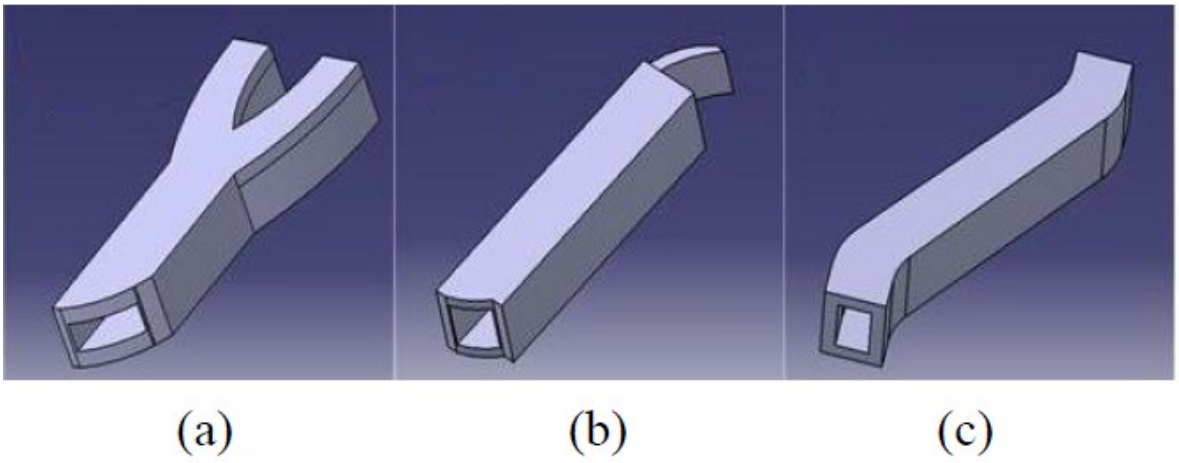

Figure 12 Model of three different types of air duct installed

Model (a) is designed in such a way so that the air introduced into the duct is divided into two and supplied to the front and side surfaces of the tire. Model (b) is a straight line, and the air is transmitted well to the tire without a significant flow resistance in the duct. However, a flow guide plate is installed at the outlet to induce air flow toward the front of the tire. In the model (c) case, it is designed in a bent shape so that air flows in from the center of the front bumper and is supplied to the front of the tire. Each duct has an inlet area of 6,000mm^2 and an outlet area of 5,000mm^2.

For comparison of various analysis results, the amount of heat generated by friction between the tire and the road according to the change in driving speed (60, 80, 100, 120 km/h) was considered.

When looking at the flow that flows through the duct and goes out of the tire, I-type has the largest number of outgoing streamlines, followed by Y-type and S-type streamlines, proportional to the tire cooling effect. Figure 13 shows the temperature distribution at each point of the tire surface with (a) basic vehicle, (b) Y-shaped, (c) S-shaped, and (d) I-shaped ducts, respectively. The running speed was 120 km/h, and when the ambient temperature around the tire was 35°C, the minimum tire surface temperature was 42°C to 52°C. The average tire temperature in the configurations with ducts was lower than that of the basic configuration. This indicates that the airflow around the tire is adequate for cooling the tire.

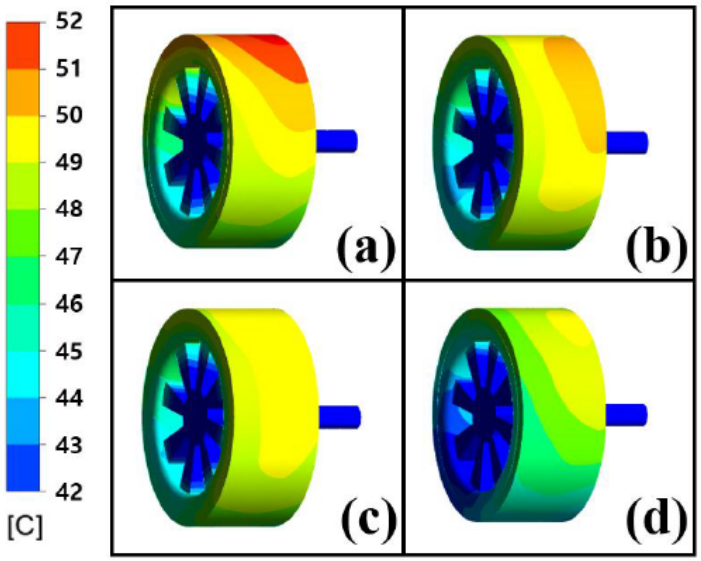

Figure 13 Temperature distribution of the tire surface with (a) basic vehicle, (b) Y-shaped, (c) S-shaped, and (d) I-shaped ducts, respectively

Figure 14 is the result of summarizing the average temperature of the tire surface by a vehicle driving speed in each case. It is found that the cooling efficiency is the best when cooling using an I-type duct, and the tire temperature tends to be lowered by 2~3℃ on average compared to the case without cooling (basic vehicle). It can be understood that the amount of scattering dust generated due to tire wear is proportional to the vehicle speed and the temperature of the tire, so it can be stated that the lower the tire temperature, the lower the amount of scattering dust. In the case of the Y-type, the outlet is divided into two branches for additional cooling of the brake pad, and the air flow to the tire is relatively reduced, so it is considered that the cooling effect is less than that of the I-type. Therefore, the lower the running speed and the lower the ambient temperature, the lower the tire surface temperature.

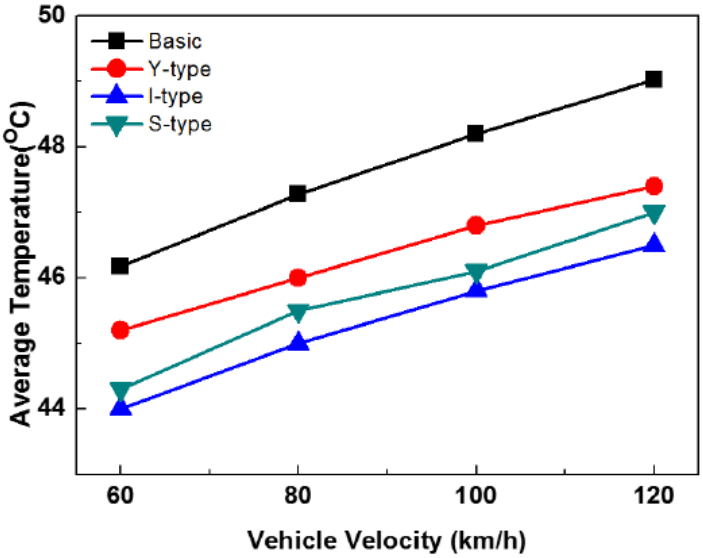

Figure 14 Average temperature of tire surface for four different vehicle configurations at different velocities

Figure 15 shows the amount of fine dust reduction compared to the basic model. The generation of fine dust increases linearly as the vehicle speed increases, and the generation of fine dust decreases when the tire is cooled using an air duct. When an I-type air duct is used, the cooling efficiency of the tire is the best, and as a result, the amount of fine dust generated due to tire wear is reduced by 4.6% on average compared to the basic type. Implementing such a solution can reduce around 0.5 kg of PM2.5 emissions generated from tire wear in a month.

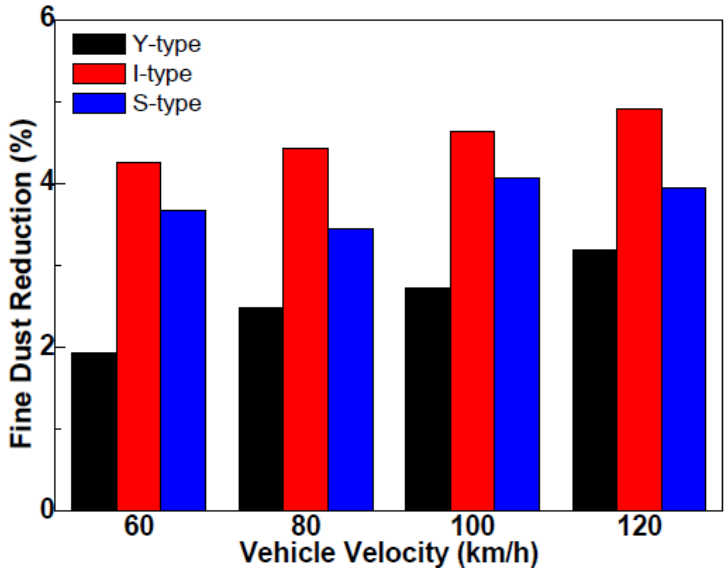

Figure 15 Fine dust reduction for four different vehicle configurations at different velocities

6.1. 2 Improvement in the asphalt materials

Vieira & Lundberg (2019) suggested that one possible solution to reduce noise and PM10 resulting from tire-pavement interaction is to use a porous pavement surface. A porous surface will reduce noise by decreasing air pressure gradients in the tire-pavement contact, lessening the road surface's acoustic impedance, and reducing the horn effect. At the same time, reducing noise and other functional aspects of such pavement would be reducing abrasion wear, which impacts air pollution through generation and suspension of particles, friction, and rolling resistance. The behavior of a Double-Layered Porous Asphalt (DLPA) was applied in the streets in the city of Linköping, Sweden, and compared to a non-porous Stone Mastic Asphalt (SMA) pavement. The acoustic analysis is combined with analyses of air quality measurements of PM10 from two Tapered Element Oscillating Microbalance (TEOM) measurement stations placed near each different pavement section. The initial results indicate that the porous pavement results in a noise reduction of up to 5 dB for light vehicles and up to 4 dB for heavy vehicles at the maximum legal speed allowed for that road section (70 km/h). Furthermore, the DLPA shows approximately 52% lower PM10 concentrations than the SMA.

The road section under study consists of a DLPA pavement with a 25 mm thick top layer and 55 mm bottom layer, with a maximum aggregate size of 11 and 16 mm, respectively, with a designed air voids content of 25%. The road section is approximately 600 m long and has average annual daily traffic (AADT) of 14,700 vehicles, of which 7% are heavy vehicles. To evaluate air quality (AQ), two air quality monitoring stations were placed are 350 miles distances, one at each type of pavement. The stations were equipped with TEOMs (Tapered Element Oscillating Microbalance) to measure PM10 concentration.

The air quality results are presented in Figure 16, showing a clear difference between the two locations. The DLPA site has clearly lower PM10 than the SMA, especially on occasions with high particle concentrations. The red line on Figure 16 marks the European Union air quality directive limit value for PM10. On average, the quotient between the DLPA and the SMA was about 52%. This shows that the DLPA location demonstrates a large degrease of PM10 compared to the SMA site. This is due to the storage capability of dust inside the porous pavement, thus trapping particles otherwise suspended by traffic at the dense pavement and clogging the DLPA.

This study by Vieira and Lundberg (2019) also noted mentioned that PM10 is influenced by meteorological conditions, like humidity, background sources as well as vehicle properties, e.g., use of studded tires, and that some of the observed decreases can be due to other aspects than porosity e.g., road surface moisture and wind direction.

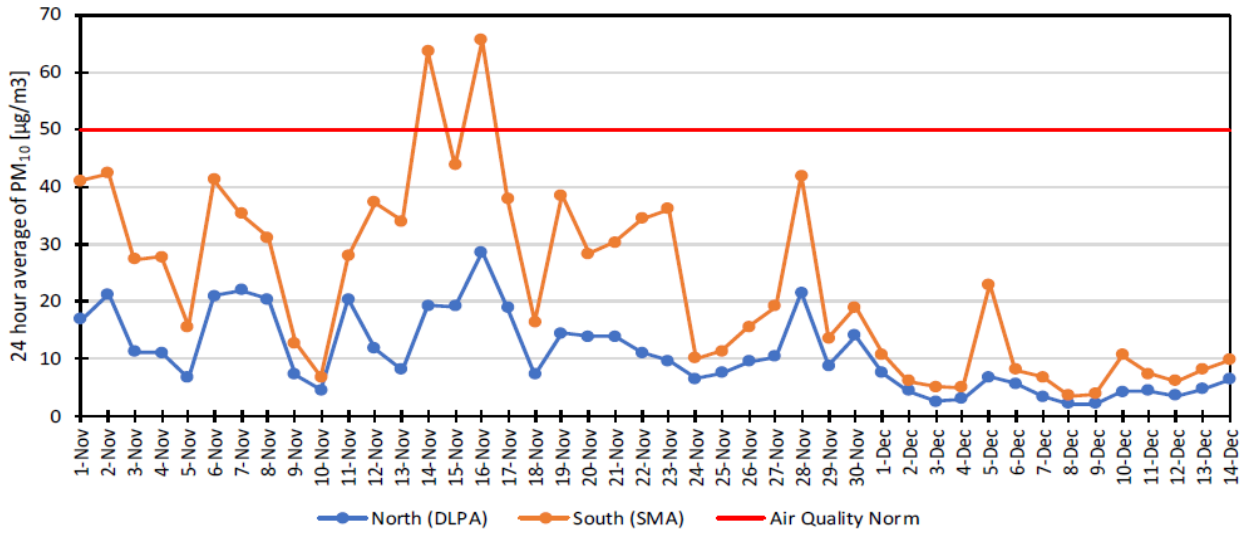

Figure 16 The 24-hour average of PM10 concentrations for a limited period in 2018 at Sweden

6.1.3 Regenerative braking system

Regenerative braking systems (RBS) are energy recovery mechanisms that slow a vehicle by converting its kinetic energy into a form that can be either used immediately or stored until needed. In these systems, the electric motor uses the vehicle's momentum to recover energy that would be otherwise lost to the brake discs as heat. This contrasts with friction braking systems, where the excess kinetic energy is converted to heat by friction in the brakes. In addition to improving the vehicle's overall efficiency, RBS can significantly extend the life of the braking system, as its parts do not wear as quickly. The amount of regenerative energy produced by a system is strictly related to the maximum power of the installed electric motor(s) and electronics and the battery's capacity to receive the energy without degrading. Above a specific battery size, the energy of a braking event can be recovered unless the battery is still fully charged. Therefore, it is safe to assume that fully electric vehicles have extremely low brake emissions (the conventional brake pads are used mainly to keep the vehicle at a standstill). Hybrid vehicles also have relatively low brake wear emissions, proportional to the level of hybridization (micro hybrids show practically no advantage from this point of view since the added mass is likely to compensate for the reduced energy to be dissipated). Vice versa, for RBS-equipped vehicles with large batteries, vehicle mass has a low to negligible influence on brake wear. While regenerative braking can be sufficient for most daily use brake applications, the combined use of regenerative braking and friction braking will remain necessary in the future for safety reasons (AUDI AG, 2016), as emergency stops still require the use of the latter.

Several estimates of the impact of RBS on brake wear PM emissions exist in the literature. Van Zeebroeck & De Cuester (2013) assumed that regenerative braking should reduce the PM emissions associated with brake wear by 50%. Timmers & Achten (2016) assumed zero brake wear emissions from RBS-equipped vehicles, and Barlow (2014) also suggested that regenerative braking produces virtually no brake wear. Hooftman et al. (2016) stated that EVs require about two-thirds (66%) less braking activity than ICEVs due to RBS. Their analysis is based on the service times of brake pads on Teslas, BMW i3s, and Nissan Leafs, which demonstrates that, on average, the brake pads of these EVs last roughly two-thirds longer than those on diesel/petrol vehicles. They noted that this outweighs the additional wear due to the vehicle's mass. Suppose the light-duty fleet of the City of Vancouver is fully converted to vehicles with RBS capability. In that case, it could potentially reduce 1.15 kg of PM2.5 and 9.15 kg of PM10 emissions per month resulting from brake wear.

The share of non-exhaust emissions from brake wear falls sharply for EVs relative to ICEVs due to regenerative braking. Although regenerative braking systems are one of the most promising technologies for reducing non-exhaust emissions from brake wear in terms of cost-effectiveness, they are currently only used in electric and hybrid-electric vehicles. Therefore, although electric vehicle manufacturers are constantly developing more technologically advanced and lightweight RBS, the penetration of these systems in vehicle fleets will grow only as fast as that of electric and hybrid-electric vehicles. For this reason, the industry should be encouraged to explore the extent to which RBS could be easily incorporated in ICEVs, e.g., via kinetic energy recovery systems. However, some trade-offs of RBS have been pointed out. If friction brake systems on vehicles with RBS are slow to reach bedded conditions, this could increase brake wear emissions when used. Additionally, if brake disc pads are degraded with the little use they receive in conjunction with RBS, rusted surfaces could lead to poor bedding conditions and higher brake wear.

6.1.4 Driving behavior

Chasapidis et al. (2018) examined brake wear particle emissions of a minivan running on a chassis dynamometer using a custom sampling system, positioned close to the braking system, under different initial speeds (30 km/h and 50 km/h), deceleration rates (0.5 m/s^2, 1.5 m/s^2, 2.5 m/s^2), and ambient temperatures (0 °C, 15 °C, and 25 °C). The selection of driving conditions was made in such a way to represent better driving conditions met in urban environments because the contribution of brake wear is more significant in big cities and urban sites. Braking from 50 km/h to full stop results in 40–100% more particles compared to 30 km/h, depending on the deceleration rate. A lower deceleration rate results in more particles being released due to the

higher contact time of the disc/pad. This fact could be useful for future speed limit legislation within urban areas.

Figure 17 shows particulate number (PN) concentration, brake pressure, and wheel speed over time of the different testing cycles zoomed at a section between the 10th and 15th braking out of 20 of each cycle. It can be seen from the PN concentration curves how brake wear particles are released at different braking patterns and wheel accelerations. For example, at softer braking (0.5 m/s^2), both at 50 km/h and 30 km/h initial speed, a single brake event reveals a clear twin peak PN concentration curve, the first at acceleration phase and the other during brake application. At 30 km/h and 2.5 m/s^2, a single sharp curve can be seen at brake application, while at 50 km/h and 2.5 m/s^2 a more spread curve without distinct peaks is obtained.

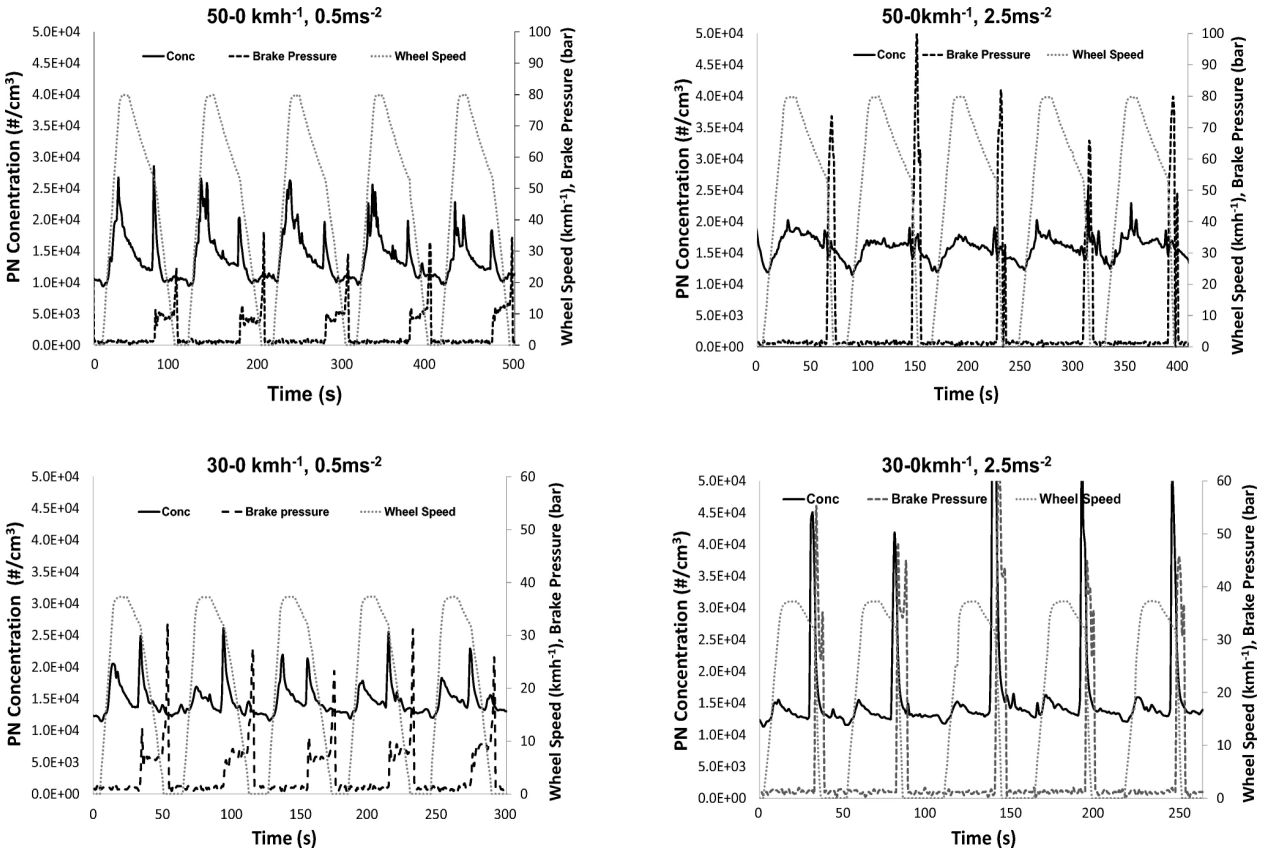

Figure 17 PN concentration, wheel speed, and brake pressure over time for the four different braking cycles. The graphs show 5 (out of 20) braking events

Regarding the PN distribution, higher temperatures of the pad result in a bimodal distribution, with the first peak being at approximately 1 µm and the second falling at the nanometer scale at about 200 nm, as shown in Figure 18. This study demonstrates that when brake pad temperature is higher than 140 °C, a clear second peak at the nanoparticle size range appears, even if high nanoparticle production has been linked with brake pad temperatures higher than 180 °C. Although it is not common to heat the brake pad material at these high temperatures under normal urban driving, aggressive driving or driving in hilly areas may do. Several toxicological studies have shown that particles in the nanometer scale are hazardous as they can enter the bloodstream through the lungs (Oberdörster, Oberdörster, & Oberdörster, 2005). Furthermore, metallic brake wear particles damage tight junctions within the mechanisms that involve oxidative stress (Gasser, et al., 2009); therefore, the vital point is the particle mass and particle quality (e.g., chemical composition and biological effect). Regardless of the driving conditions, a single brake event reveals a clear two-peak PN concentration curve, the first at the acceleration phase and the second during brake application.

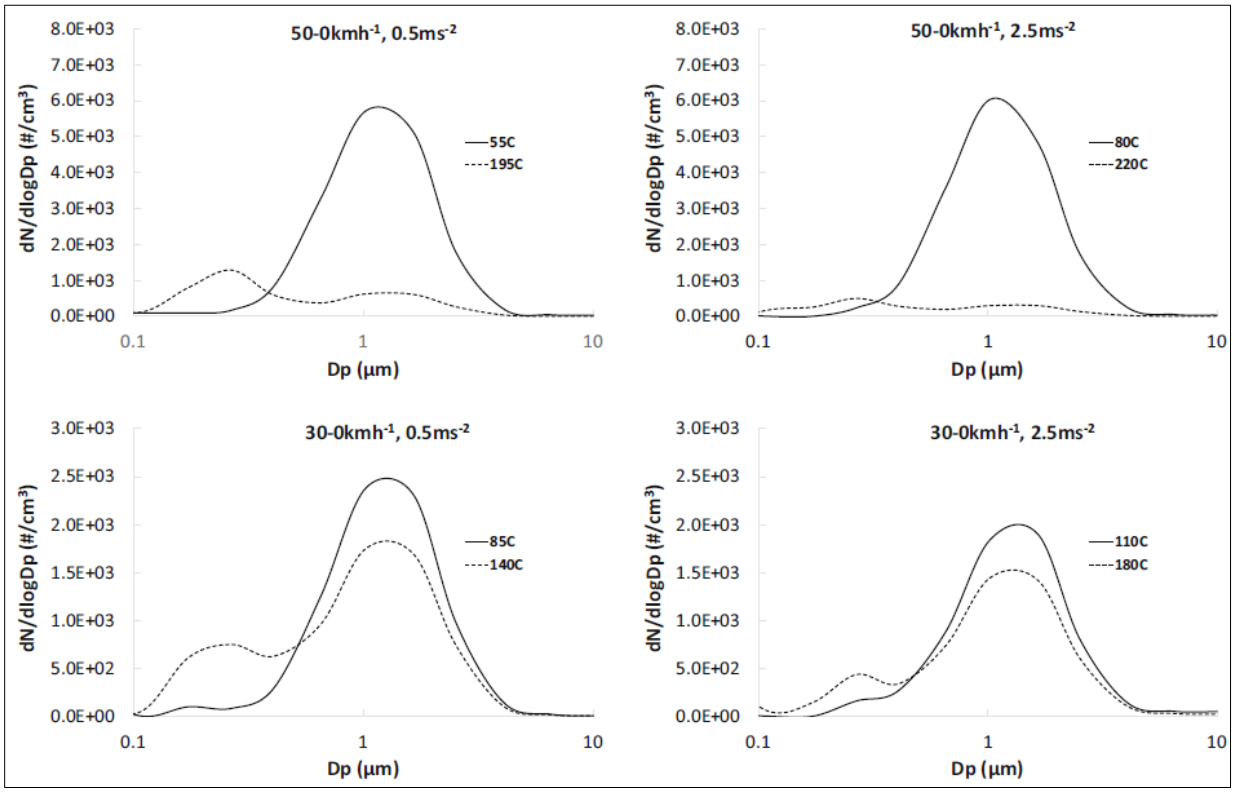

Figure 18 Particle number distributions for braking cycles at low and higher brake pad temperature

It was also found that only 9–50% of the total particles emitted are released during the braking phase, and therefore the most significant amount is released on the following acceleration phase. These are most probably particles that have been deposited in the brake system from past braking and are released due to the high-velocity flow resulting from the wheel acceleration. As shown in Figure 19, the particles emitted at each braking event are comparable for all different braking patterns; however, at the lower initial braking speed of 30 km/h, the percentage over total particles are higher. This may indicate that a higher number of smaller particles of magnetic content (i.e., Fe oxides) is emitted when a higher initial braking speed is applied. These particles are most probably attracted to the brake mechanism or the rim and released later when the wheel is accelerating (Boulter, 2005). On the other hand, only 15% of the total particles are emitted at the braking event at a higher initial speed. This can be attributed to the lower resuspension at lower wheel acceleration due to the lower swirling air flow and lower vibrations.

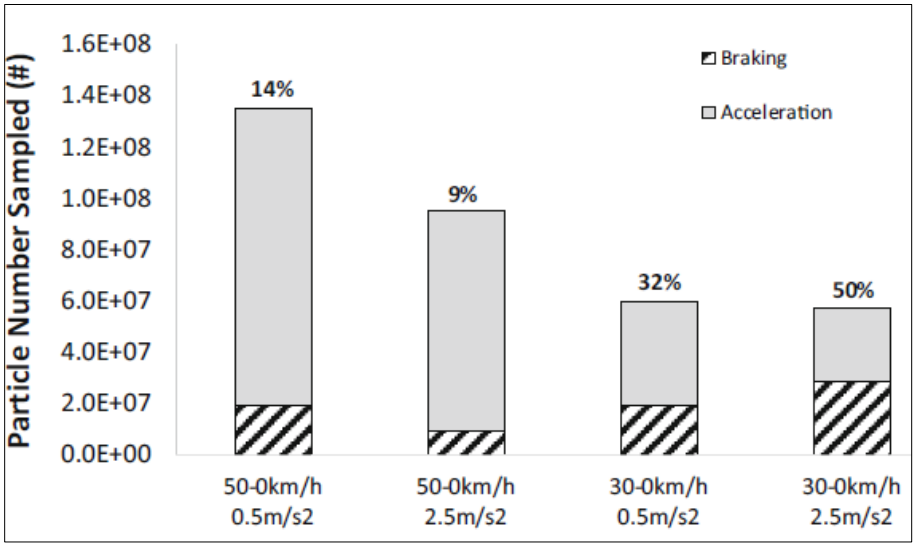

Figure 19 Particles emitted during braking phase and acceleration phase at various conditions

The ambient temperature appears to have a negligible effect on particle generation, as shown in Figure 20. Slightly lower PN concentration at lower temperatures can be attributed to the lower temperature of the pads and the disc that affect wear particle production. Generally, lower emissions at lower ambient temperatures can be explained by the thermophoresis phenomenon. A larger temperature gradient of the emission surfaces (pad/disc) and the surrounding air and surfaces (caliper, wheel, etc.) can result in larger forces to airborne particles towards the colder surfaces. Therefore, fewer particles can travel beyond the vehicle wheel and be released into the environment.

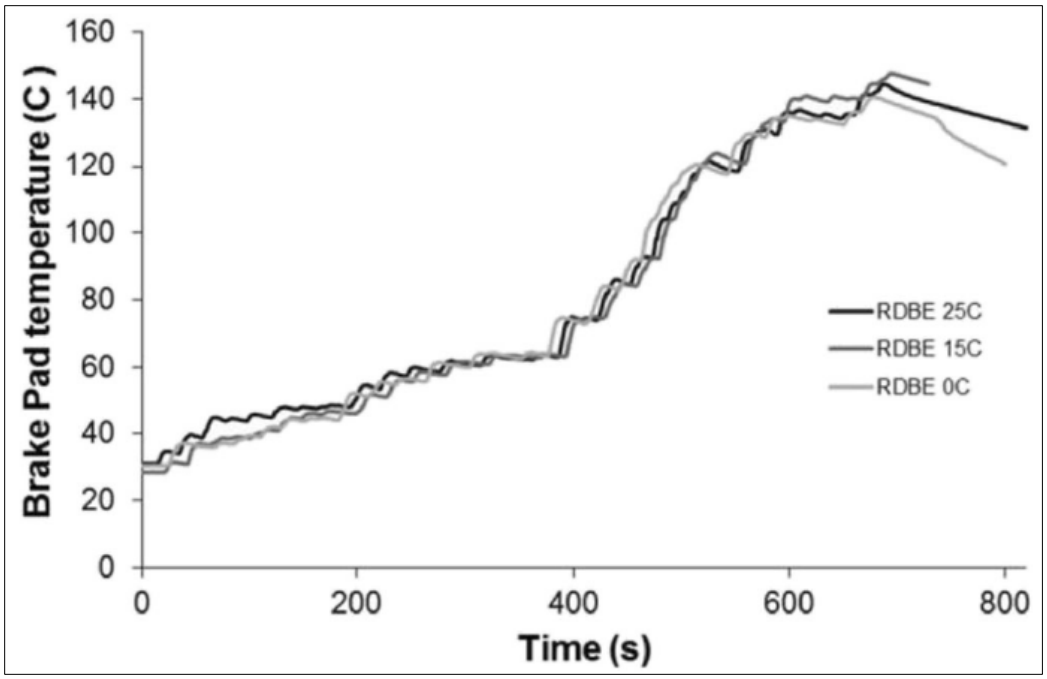

Figure 20 Brake pad temperature over time for a braking cycle representing real-world urban driving performed at 0 °C, 15 °C, and 25 °C

6.1.5 Impact of electric vehicles

Electric vehicles were proposed as a potential technological solution to urban air pollution. The absence of tailpipe emissions reduces nitrogen oxides (NO_x) and other exhaust pollutant emissions in urban areas. However, the impact of pollutants emitted during the production of the electricity needed to fuel the battery must also be considered. As for NO_x in particular, the overall emission factor for EVs is expected to be far lower than combustion engine cars since EVs can exploit the excess of electricity produced by photovoltaic and wind power plants (Richardson, 2013).

However, EVs contribute to air pollution through non-exhaust emissions (NEE) of particulate matter. Hence, they cannot be defined as 'zero-emission vehicles' but rather 'zero exhaust emission vehicles' (AQEG, 2019). As well as emissions from conventional fossil fuel-powered cars, NEE from electric vehicles can be mainly ascribed to tire and road wear and dust resuspension. Brake wear emissions for hybrid and full-electric vehicles are estimated to be lower than combustion engine cars thanks to the regenerative braking systems (RBS) in addition to conventional frictional brakes.

On the other hand, tire and road wear and resuspended dust emission are expected to be higher for EVs because of their increased weight. There is a positive relationship between vehicle weight

and non-exhaust emissions, especially for PM deriving from dust resuspension (Garg, et al., 2000; Timmers & Achten, 2016). As highlighted by several authors, EVs are heavier than their counterparts with an internal combustion engine (ICE). For example, Moawad, Sharer, & Rousseau (2013) estimated that EVs are between 43% and 56% heavier than ICE vehicles. In contrast, Bauer, Hofer, Althaus, Del Duce, & Simons (2015) and Timmers & Achten (2016) found the weight increase to be 24%. Moreover, Burnham (2012) estimated that the weight of electric cars and SUVs is 43% and 52% higher than their ICE counterparts, respectively. The higher weight is expected to compensate for the absence of tailpipe emissions, thus leading to comparable primary PM emission factors for EVs and ICE vehicles. As an example, Timmers & Achten (2016) estimated that the additional weight due to vehicle electrification leads to an overall increase of NEE equal to 12.1 mg km^{-1} veh^{-1} for PM10 (corresponding to an increase of 1.1 mg km^{-1} veh^{-1} for tire wear, 1.4 mg km^{-1} veh^{-1} for road wear and 9.6 mg km^{-1} veh^{-1} for resuspended dust) and 4.4 mg km^{-1} veh^{-1} for PM2.5 (corresponding to an increase of 0.8 mg km^{-1} veh^{-1} for tire wear, 0.7 mg km^{-1} veh^{-1} for road wear and 2.9 mg km^{-1} veh^{-1} for resuspended dust). This increase substantially compensates the particulate emission saving induced by the diesel/gasoline-to-electric transition, which is estimated to be equal to 12.4 mg km^{-1} veh^{-1} for PM10 (3.1 mg km^{-1} veh^{-1} for tailpipe and 9.3 mg km^{-1} veh^{-1} for brake wear) and to 5.2 mg km^{-1} veh^{-1} for PM2.5 (3 mg km^{-1} veh^{-1} for tailpipe and 2.2 mg km^{-1} veh^{-1} for brake wear).

There are several options for future policy that have the potential to reduce non-exhaust emissions. A good start would be to create maximum limits for non-exhaust emissions that all new vehicles (ICEVs and EVs) need to comply with. However, measurements of non-exhaust emissions so far have produced divergent results, depending on the measurement method used. So, to introduce non-exhaust limits, a standardized measurement method needs to be introduced. Further improvements can be made by encouraging innovation in reducing vehicle weight. EV technology such as lightweight body design, improved tire design, and regenerative brakes could all be applied to ICEVs to decrease their non-exhaust emissions further. Finally, it is recommended that governments create incentives for consumers and car manufacturers to switch to more lightweight passenger cars to reverse the trend of increasing vehicle weight in all market segments (Timmers & Achten, 2016).

6.2 Prevention strategies

Non-technological prevention strategies entail a wide variety of solutions for the reduction of the overall traffic volume (fuel and vehicle taxation, road traffic management policies, etc.), the renewal and transformation of urban vehicle fleets, and the improvement of public transport and urban planning (pedestrians and green areas, cycle lanes, low emission zones). For example, cleaning procedures can be imposed for vehicles exiting construction sites, waste-management plants, and similar places, which, otherwise, would bring large quantities of dust on the road.

The imposition of speed limits and the promotion of a smooth driving style reduce braking events and dust resuspension, thus improving passenger safety and air quality (Gustafsson, et al., 2008; Querol Carceller, Amato, Robusté Antón, Holman, & Harrison, 2018). For instance, Kwak, Kim, Lee, & Lee (2013) observed a significant increase in PM concentrations of both road wear and tire wear particles during deceleration events. Since both the amount and size of the generated particles strongly depend on the intensity and duration of the braking events, brake wear emissions were found to be also influenced by the driving style. Stronger and longer braking events produce higher disk temperatures which, in turn, induce the generation of a large amount of fine and ultrafine particles (Garg, et al., 2000; Nosko & Olofsson, 2017; Wahlström, Olander, & Olofsson, 2012).

Tian et al. (2021) has discovered the lethal effect of the chemical named 6PPD on Coho Salmon. Hence, the tire manufacturers should be enforced to produce tires without this chemical, which is used as a tire rubber antioxidant. Once the modified tires become available, the City of Vancouver needs to change the tires of its fleet to the revised version.

6.3 Mitigation strategies

Mitigation measures to reduce resuspendable dust are sweeping, street washing, sediment removal, and dust suppressant. Street sweeping reduces the quantity of dust on the streets and, hence, the fugitive dust that can be re-entrained into the atmosphere by car traffic. The most common types of sweeping vehicles are mechanical broom sweepers, regenerative-air sweepers, and vacuum sweepers (Amato, Querol, Johansson, Nagl, & Alastuey, 2010; Kang, Debats, & Stenstrom, 2009). More specifically, mechanical broom sweepers collect debris into a hopper through a pickup broom. Regenerative air-sweepers are instead equipped with a gutter, which directs the materials toward a pickup head, while air is blown onto the pavement to dislodge particles entrained within cracks. Vacuum sweepers are equipped with gutter brooms and strong vacuum heads to collect large and small debris (Calvillo, Williams, & Brooks, 2015).

Street sweeping is a traditional method adopted in most cities for centuries, but investigations on their impact have been carried out only over the last 40 years. Some researchers analyzed both standard mechanical street brooms and air-regenerative sweepers for a wide range of cleaning frequencies and street textures to understand the impact of the practices on surface water quality. The evaluation of the sweeping street efficiency was obtained through stormwater quality assessment pre- and post-sweeping. The first studies on the matter were conducted as part of the Nationwide Urban Runoff Program (NURP), which concluded that street sweeping was largely ineffective at reducing the mean concentration of pollutants in urban runoff during a rain event (Pitt, 1979; USEPA, Results of the Nationwide Urban Runoff Program. Volume I- Final Report, 1983). Subsequent studies questioned the NURP conclusions due to the development of sweepers with the ability to retain finer particles (PM10) with specific filtering mechanisms (Amato, Querol, Johansson, Nagl, & Alastuey, 2010). Indeed, more recent research projects reported quantitative evidence that street sweeping directly improves runoff water quality (Curtis, 2002; Martinelli, Waschbusch, Bannerman, & Wisner, 2002). As an example, Selbig (2016) demonstrated a significant reduction in mean total suspended solids concentrations in samples collected from a gutter of a street swept by a mechanical sweeper (74% of reduction) and a vacuum sweeper (85%).

However, there is still considerable uncertainty about pollutant reduction efficiencies, which are extremely variable depending on the frequency and timing of sweeping between storms and the high variability of stormwater quality loads (Hixon & Dymond, 2018). Regardless, all the different street sweeping techniques proved to be more efficient for removing non-resuspendable coarser particles. Although this may seem negligible from the point of view of air quality, it should be remembered that fine particles also originate from the fragmentation of the coarser ones. For this reason, the utility of this traditional cleaning technique should not be underestimated (Amato, Querol, Johansson, Nagl, & Alastuey, 2010).

Another mitigation measure is water flushing, which consists of a water jet – generally applied in combination with street sweeping – to remove residues from street surfaces. Since the water jet alone cannot easily move the dust toward the sewage system unless an intense water flow is applied, no significant and long-lasting differences were found in PM10 concentrations after applying this technique (Norman & Johansson, 2006). Other studies analyzed the combined effect on urban air quality of street sweeping and water flushing. Chang, Chou, Su, & Tseng (2005) tested a combination of modified regenerative-air vacuum sweeper and washer, observing a short-term (3–4 h) direct impact on ambient PM emissions. More recently, Kryłów & Generowicz (2019) observed a 17.3% reduction of PM10 and a 15.4% reduction of PM2.5, which lasted up to three days after sweeping and street washing in Kraków, Poland. However, they observed a short-term

negative effect due to an increase of PM concentration during the street cleaning due to traffic jams and dust resuspension. Nevertheless, the overall impact of street sweeping and washing proved positive.

Dust suppressants can be instead classified, according to their chemical composition, as surfactants, salts, polymers, resins, and bitumen. These chemicals are water-soluble and are spread on the road in a water mixture. They form a film on the particles, which induces the reduction of water evaporation rate and the absorption of moisture from the air, thus resulting in the dust attachment to the road (Gulia, Goyal, Goyal, & Kumar, 2019). For example, Amato et al. (2014) evaluated the effectiveness of calcium acetate and $MgCl_2$ in reducing road dust emissions in a Mediterranean city. The authors observed episodic reductions of PM after applying calcium acetate, but the results were not statistically significant or systematic.

Similarly, the application of $MgCl_2$ slightly reduced mineral and brake wear tracers. Better results were obtained in Sweden, reducing the daily mean PM10 concentration up to 35% (Norman & Johansson, 2006). Therefore, the studies carried out so far highlighted that the effectiveness of dust suppressants is strongly influenced by local conditions, such as the amount of dust and climate.

7.0 Conclusion

Non-exhaust emissions of particles apply to all forms of ground transport and can be categorized as those from four sources: brake wear, tire wear, road surface wear, and resuspended road dust. Quantitative data on the magnitude of non-exhaust emissions are sparse and highly uncertain, particularly when compared to data for exhaust emissions. Emissions vary widely according to brake, tire, and road surface material and with driving style. The emission factor calculation methodology for NEE has not evolved in time as to vehicle designs, in contrast to the regularly updated emissions factors used for exhaust emissions. Consequently, emission factors that exist for NEE have a wide range of uncertainty. Min-max uncertainty ranges spanning a factor of two or more are typical. This study utilized the method utilized by the USEPA, which was last updated in November 2020, for quantifying the NEE from the light-duty fleet of the City of Vancouver.

Acknowledging the considerable uncertainties, it is estimated that the NEE particles from brake wear, tire wear, and road surface wear now constitute the majority source of primary particulate matter (by mass) from road transport, in both PM2.5 and PM10 size fractions. These proportions are set to become even more dominant in the future with continued projected declines in vehicle-fleet exhaust PM emissions. The available data indicate that NEE is especially important in urban environments due to greater braking per km than non-urban roads. Tire wear emissions are estimated to be greatest on high traffic volume trunk roads and motorways (urban and rural).

Increases in vehicle mass generally increase NEE, which may have implications for electric vehicles if they are heavier than the conventional diesel and petrol-fueled models they replace because of battery mass. To any vehicle with a heavier powertrain, the equivalent internal combustion engine vehicle. The same applies to autonomous vehicles, which are also heavier than equivalent human-driven vehicles. Regenerative braking does not rely on frictional wear of brake materials, so vehicles using this braking system have lower brake wear emissions. However, the net balance between reductions in brake wear emissions and potential increases in tire and road wear emissions and resuspension for vehicles with regenerative braking remains unquantified. It will depend upon road type and the driving mode, as both influences the balance between the different sources of emissions.

At present, there is no type of approval legislation in Canada covering non-exhaust emissions, nor product standards governing the composition of brake systems and tires that are designed explicitly to limit air pollution. Methods of measuring NEE presently lack international consistency. Efforts are ongoing to develop testing approaches that reflect real-world driving conditions.

References

Almeida, S., Manousakas, M., Diapouli, E., Kertesz, Z., Samek, L., Hristova, E., . . . Eleftheriadis, K. (2020). Ambient particulate matter source apportionment using receptor modelling in European and Central Asia urban areas. *Environ. Pollut., 266, Article 115199*.

Amato, F., Cassee, F. R., Denier van der Gon, H. A., Gehrig, R., Gustafsson, M., Hafner, W., . . . Querol, X. (2014). Urban air quality: the challenge of traffic non-exhaust emissions. *J. Hazard. Mater., 275*, pp. 31-36.

Amato, F., Karanasiou, A., Cordoba, P., Alastuey, A., Moreno, T., Lucarelli, F., . . . Querol, X. (2014). Effects of road dust suppressants on PM levels in a mediterranean urban area. *Environ. Sci. Technol., 48*, pp. 8069-8077.

Amato, F., Pandolfi, M., Escrig, A., Querol, X., Alastuey, A., Pey, J., . . . Hopke, P. (2009). Quantifying road dust resuspension in urban environment by multilinear engine: a comparison with PMF2. *Atmos Environ 43*, pp. 2770–2780.

Amato, F., Querol, X., Johansson, C., Nagl, C., & Alastuey, A. (2010). A review on the effectiveness of street sweeping, washing and dust suppressants as urban PM control methods. *Sci. Total Environ., 408*, pp. 3070-3084.

Anenberg, S. C., West, J. J., Yu, H., Chin, M., Schulz, M., Bergmann, D., . . . Takemura, T. (2014). Impacts of intercontinental transport of anthropogenic fine particulate matter on human mortality. *Air Quality, Atmosphere & Health, 7*, pp. 369-379.

AQEG. (2019). *Non-Exhaust Emissions from Road Traffic.* London: Air Quality Expert Group.

AUDI AG. (2016). *Internal investigations of braking systems for plug-in hybrid electric vehicles.*

Barlow, T. (2014). *Briefing paper on non-exhaust particulate emissions from road transport.* Transport Research Laboratory.

Bauer, C., Hofer, J., Althaus, H.-J., Del Duce, A., & Simons, A. (2015). The environmental performance of current and future passenger vehicles: life cycle assessment based on a novel scenario analysis framework. *Appl. Energy, 157*, pp. 871-883.

Boulter, P. (2005). *A review of emission factors and models for road vehicle non-exhaust particulate matter.* Wokingham: TRL Report PPR065.

Brauer, M., Amann, M., Burnett, R., Cohen, A., Dentener, F., & Ezzati, M. (2012). Exposure assessment for estimation of the global burden of disease attributable to outdoor air pollution. *Environ. Sci. Technol., 46*, pp. 652-660.

Bukowiecki, N., Gehrig, R., Lienemann, P., Hill, M., Figi, R., & Buchmann, B. (2009). *PM10 emission factors of abrasion particles from road traffic (APART).* Swiss Association of Road and Transportation Experts (VSS).

Bukowiecki, N., Lienemann, P., Hill, M., Furger, M., Richard, A., Amato, F., . . . Gehrig, R. (2010). PM10 emission factors for non-exhaust particles generated by road traffic in an urban street canyon and along a freeway in Switzerland. *Atmos. Environ., 44*, pp. 2330-2340.

Burnham, A. (2012). *Updated Vehicle Specifications in the GREET Vehicle-Cycle Model.* Illinois: Argonne National Laboratory.

Calvillo, S. J., Williams, E. S., & Brooks, B. W. (2015). Street dust: implications for stormwater and air quality, and environmental management through street sweeping. *Rev. Environ. Contam. Toxicol., 233*, pp. 71-128.

Candeias, C., Vicente, E., Tomé, M., Rocha, F., Ávila, P., & Alves, C. (2020). Geochemical, mineralogical and morphological characterisation of road dust and associated health risks. *Int. J. Environ. Res. Public Health, 17 (5), Article 1563*.

Chang, Y., Chou, C., Su, K., & Tseng, C. (2005). Effectiveness of street sweeping and washing for controlling ambient TSP. *Atmos. Environ., 39*, pp. 1891-1902.

Curtis, M. (2002). *Street Sweeping for Pollutant Removal. Watershed Management Division, Department of Environmental Protection, Montgomery County, MD.* Maryland.

Denby, B., Kupiainen, K., & Gustafsson, M. (2018). Chapter 9- review of road dust emissions. In Amato F, *Non-Exhaust Emissions.* (pp. pp. 183-203). Academic Press.

EEA. (2019). *EMEP/EEA Air Pollutant Emission Inventory Guidebook 2019.*

European Community. (2008). Directive 2008/50/EC of the European Parliament and of the Council of 21 May 2008 on ambient air quality and cleaner air for Europe. *Off. J. Eur. Union, 029*, pp. 169-212.

Faino, M. (2018). *Tyre and Road Wear Particles: The Tyre Industry Perspective.* UN WP29 GRPE PMP-48-13.

Garg, B. D., Cadle, S. H., Mulawa, P. A., Groblicki, P. J., Laroo, C., & Parr, G. A. (2000). Brake Wear Particulate Matter Emissions. *Environmental Science and Technology, 34(21)*, pp. 4463-4469.

Gasser, M., Riediker, M., Mueller, L., Perrenoud, A., Blank, F., Gehr, P., & Rothen-Rutishauser, B. (2009). Toxic effects of brake wear particles on epithelial lung cells in vitro. *Fibre Toxicol*, pp. 1-13.

Gehrig, R., Zeyer, K., Bukowiecki, N., Lienemann, P., Poulikakos, L., Furger, M., & Buchmann, B. (2010). Mobile load simulators – a tool to distinguish between the emissions due to abrasion and resuspension of PM10 from road surfaces. *Atmos. Environ., 44*, pp. 4937-4943.

Gulia, S., Goyal, P., Goyal, S. K., & Kumar, R. (2019). Re-suspension of road dust: contribution, assessment and control through dust suppressants—a review. *Int. J. Environ. Sci. Technol., 16*, pp. 1717-1728.

Gustafsson, M., Blomqvist, G., Gudmundsson, A., Dahl, A., Swietlicki, E., Bohgard, M., . . . Ljungman, A. (2008). Properties and toxicological effects of particles from the interaction between tyres, road pavement and winter traction material. *Sci. Total Environ., 393 (2–3)*, pp. 226-240.

Harrison, R. M., Jones, A. M., Gietl, J., Yin, J., & Green, D. C. (2012). Estimation of the contributions of brake dust, tire wear, and resuspension to non-exhaust traffic particles derived from atmospheric measurements. *Environ Sci Technol 46*, pp. 6523–6529.

Hixon, L., & Dymond, R. (2018). State of the practice: assessing water quality benefits from street sweeping. *J. Sustain. Water Built Environ., 4 (3)*, Article 04018007.

Hooftman, N. e. (2016). Environmental analysis of petrol, diesel and electric passenger cars in a Belgian urban setting. *Energies, Vol. 9/2*, pp. 1-24.

Hooftman, N., Messagie, M., Van Mierlo, J., & Coosemans, T. (2018). A review of the European passenger car regulations – real driving emissions vs local air quality. *Renew. Sust. Energ. Rev., 86*, pp. 1-21.

ICCT. (2021, 17 July). *European vehicle market statistics 2018/2019*. Retrieved from http://eupocketbook.theicct.org

Kang, J.-H., Debats, S. R., & Stenstrom, M. K. (2009). Stormwater management using street sweeping. *J. Environ. Eng., 135*, pp. 479-489,.

Kelly, F. J., & Fussell, J. C. (2012). Size, source and chemical composition as determinants of toxicity attributable to ambient particulate matter. *Atmos. Environ., 60*, pp. 504-526.

Kryłów, M., & Generowicz, A. (2019). Impact of street sweeping and washing on the pm10 and PM2.5 concentrations in cracow (Poland). *Rocznik Ochrona Srodowiska, 21*, pp. 691-711.

Kukutschová, J., Moravec, P., Tomášek, V., Matějka, V., Smolík, J., Schwarz, J., . . . Filip, P. (2011). On airborne nano/microsized wear particles released from low-metallic automotive brakes. *Environ Pollut 159*, pp. 998–1006.

Kupiainen, K., Tervahattu, H., Räisänen, M., Mäkelä, T., Aurela, M., & Hillamo, R. (2005). Size and composition of airborne particles from pavement wear, tyres, and traction sanding. *Environmental Science & Technology 39*, pp. 699-706.

Kwak, J.-h., Kim, H., Lee, J., & Lee, S. (2013). Characterization of non-exhaust coarse and fine particles from on-road driving and laboratory measurements. *Sci. Total Environ., 458-460*, pp. 273-282.

Lawrence, S., Sokhi, R., Ravindra, K., Mao, H., Prain, H. D., & Bull, I. D. (2013). Source apportionment of traffic emissions of particulatematter using tunnel measurements. *Atmos Environ 77*, pp. 548–557.

Lindgren, Å. (1996). Asphalt wear and pollution transport. *Science of the Total Environment, Volumes 189 - 190*, pp. 281-286.

Lowne, R. (1970). The Effect of Road Surface Texture on Tire Wear. *Wear Volume 15, Issue 1*, pp. 57-70.

Luhana, L., Sokhi, R., Warner, L., M. H., Boulter, P., McCrae, I., . . . Osborn, D. (2004). *Non-exhaust particulate measurements:results, Deliverable 8 of the European Commission DG TrEn, 5th Framework PARTICULATES project , Contract No. 2000 RD.*

Martinelli, T., Waschbusch, R., Bannerman, R., & Wisner, A. (2002). *Pollutant Loadings to Stormwater Runoff from Highways: The Impact of a Freeway Sweeping Program, Wisconsin Department of Transportation R&D Program.* Madison, Wisconsin.

Moawad, A., Sharer, P., & Rousseau, A. (2013). *Light-Duty Vehicle Fuel Consumption Displacement Potential up to 2045.* Illinois: Argonne National Laboratory (ANL).

Norman, M., & Johansson, C. (2006). Studies of some measures to reduce road dust emissions from paved roads in Scandinavia. *Atmos. Environ., 40 (32)*, pp. 6154-6164.

Nosko, O., & Olofsson, U. (2017). Quantification of ultrafine airborne particulate matter generated by the wear of car brake materials. *Wear, 374-375*, pp. 92-96.

Oberdörster, G., Oberdörster, E., & Oberdörster, J. (2005). Nanotoxicology: an emerging discipline evolving from studies of ultrafine particles. *Environ. Health Perspect. 113(7)*, pp. 823–839.

OECD. (2020). *Non-exhaust particulate emissions from road transport : An ignored environmental policy challenge.* Paris: OECD Publishing.

Pant, P., & Harrison, R. M. (2013). Estimation of the contribution of road traffic emissions to particulate matter concentrations from field measurements: a review. *Atmos. Environ., 77*, pp. 78-97.

Park, H., Cho, H., Lee, J., Kim, Y., Lee, J., & Kim, K. (2019). Tire cooling for reduction of fine dust generation. *Korean Society of Mechanical Engineers, B 43*, 677–682.

Pitt, R. (1979). *Demonstration of Nonpoint Pollution Abatement through Improved Street Cleaning Practices. Final Report.* San Francisco: US EPA.

Querol Carceller, X., Amato, F., Robusté Antón, F., Holman, C., & Harrison, R. M. (2018). Non-technological measures on road traffic to abate urban air pollution. *Academic Press*, pp. 229–260.

Richardson, D. (2013). Electric vehicles and the electric grid: a review of modeling approaches, impacts, and renewable energy integration. *Renew. Sust. Energ. Rev., 19*, pp. 247-254.

Sanders, P. G., Xu, N., Dalka, T. M., & Maricq, M. M. (2003). Airborne Brake Wear Debris: Size Distributions, Composition, and a Comparison of Dynamometer and Vehicle Tests. *Environmental Science & Technology, 37 (18)*, pp. 4060-4069.

Selbig, W. (2016). Evaluation of leaf removal as a means to reduce nutrient concentrations and loads in urban stormwater. *Sci. Total Environ., 571*, pp. 124-133.

Thorpe, A., & Harrison, R. M. (2008). Sources and properties of non-exhaust particulate matter from road traffic- A review. *Volume 400, Issues 1–3*, pp. 270-282.

Tian, Z., Zhao, H., Peter, K. T., Gonzalez, M., Wetzel, J., Wu, C., . . . Jenne. (2021). A ubiquitous tire rubber-derived chemical induces acute mortality in coho salmon. *Science (American Association for the Advancement of Science), Volume 371, Issue 6525*, pp. 185-189.

Timmers, V., & Achten, P. (2016). Non-exhaust PM emissions from electric vehicles. *Atmos. Environ., 134*, pp. 10-17.

USEPA. (1983). *Results of the Nationwide Urban Runoff Program. Volume I - Final Report.* Washington DC: US EPA.

USEPA. (1992). *Procedures of Emission Inventory Preparation - Volume IV: Mobile Sources.* Washington DC.

USEPA. (2020). *All EPA Emission Standards Light-Duty Vehicles and Trucks and Motorcycles.* Washington DC, USA.

USEPA. (2020). *Brake and tire wear emissions from on-road vehicles in MOVES3.* US Environmental Protection Agency.

Van Zeebroeck, B., & De Ceuster, G. (2013). *Elektrische auto zorgt voor evenveel fijn stof als conventionele auto.* Transport & Mobility Leuven.

Wahlström, J. (2009). *Towards a simulation methodology for prediction of airborne wear particles from disc brakes.*

Wahlström, J., Olander, L., & Olofsson, U. (2012). A pin-on-disc study focusing on how different load levels affect the concentration and size distribution of airborne Wear particles from the disc brake materials. *Tribol. Lett., 46*, pp. 195-204.

Warner, L., Sokhi, R., Luhana, L., Boulter, P., & McCrae, I. (2004). Non-exhaust particle emissions from road transport. *11th International Conference "Transport and air pollution", Dept. of Environmental Sciences. Univ. of Hertfordshire, UK.*